Hindawi
Shock and Vibration
Volume 2022, Article ID 7844875, 25 pages
https://doi.org/10.1155/2022/7844875

Research Article

Modeling of Preload Bolted Flange Connection Structure for Loosening Analysis and Detection

Weicheng Sun,[1] **Zhenqun Guan**,[1] **Yan Chen**,[2] **Jiacheng Pan**,[1] **and Yan Zeng**[1]

[1]*Department of Engineering Mechanics, Dalian University of Technology, Dalian 116024, China*
[2]*Beijing Institute of Nearspace Vehicle's Systems Engineering, Science and Technology on Space Physics Laboratory, Beijing 100076, China*

Correspondence should be addressed to Yan Zeng; zengyan@dlut.edu.cn

Received 7 January 2022; Revised 15 May 2022; Accepted 20 May 2022; Published 6 June 2022

Academic Editor: Sami El-Borgi

The specified finite element model is proposed for preload bolted flange connection structure widely used in aerospace and rocket design. A fine hexahedral mesh model of the bolt is used to predict the dynamic response of the structure accurately. The tightening process, which is ignored in the traditional I-shaped simplified model of bolted flange connection structure, can be simulated well based on the proposed model. After the vibration analysis and stress analysis of the bolted flange connection structure under impact load, it is found that the change of contact state of the flange surface results in a larger sticking contact area. And the reduction of the contact area at the thread causes slippage when the bolt is loose. As bolt loosening leads to changes in the time and frequency domain of response, a new loosening detection method for the preload bolted flange connection is provided. The index for identifying the loosening is designed using empirical mode decomposition and discrete integral in the high-frequency domain. The experiment of the preload bolted flange connection structure under impact load shows the efficiency of the proposed method which can identify loosening based on acceleration signal quickly and nondestructively.

1. Introduction

The bolted flange connection is often used in aircraft and rocket interstage structures, and its mechanical properties are complex under various operating settings and equipment conditions. Although the use of bolted flange connections can stiffen the connected structures, the discontinuity of the structure in the bolted flange connections results in some nonlinear properties that affect the structural safety and reliability.

Suitable models can help us understand the nonlinear features of the bolted flange connection structure under various loads. In 2007, Kim et al. [1] compared a variety of bolt modeling methodologies to analyze bolted flange structures [1]. Luan et al. [2] introduced a simplified model of the bolted flange connection with bilinear stiffness to reveal the relationship between the structure's transversal and longitudinal coupling vibration [2]. Expanding the work of Luan et al. [2], Lu et al. [3] studied the coupling vibration of the bolted flange connection structure with shear pins to give applicable advice in the design of connection structures [3]. Tian et al. [4] proposed the simulation method and corresponding experiment of impact failure of bolted flange connection structure in the rocket [4]. Zhu et al. [5] considered the nonlinear and inelastic behavior of the gasket in the finite element simulation of the tightening process of bolted flange connection structure. They evaluated the dispersion of the bolt pretightening force generated during the tightening sequence, to improve the safety and reliability of the structure [5]. Guo et al. [6] studied the characteristics of frequency variation in the responses of bolted flange structures under different impact loads [6]. Tang et al. [7] established a simplified model of the bolted joined cylindrical shell structure based on the Sanders shell theory [7] and analyzed the dynamic and nonlinear characteristics [8]. Then they proposed a microslip model to reproduce the friction on the interface [9, 10]. Jamia et al. [11] established a beam element equivalent model to study the microslip

behavior of the bolted flange connection structure [11]. Meisami et al. [12] developed a beam-spring model of the connection structure based on the Euler-Bernoulli theory to simulate the structural dynamic behavior. Beaudion and Behdinan [13] proposed a new spigot flange model with the bilinear stiffness springs for friction analysis according to the experiments. Li et al. [14] proposed a simplified dynamic modeling method based on structural static analysis to simulate the dynamic response of a launch vehicle's nonlinear bolted flange joint. Jiang et al. [15] discovered that the contact condition of the bolted flange connection structure is associated with the preload of the bolt. Nassar and Housari [16] investigated certain aspects affecting the self-loosening of threaded fasteners, such as thread fit, thread pitch, and initial tension, using a basic mathematical model and experiments [16, 17]. Then they provided a more precise mathematical model to forecast the preload variation throughout the self-loosening process by looking at the link between the thread friction torque and pitch torque components [18]. Above all, the current analysis mainly aims to analyze and design limited local parameters of the bolted flange connection structures. There are still many works to do in the future for the influence of dynamic working conditions and the preload on the overall connection structure. In particular, the existing works on the simplified modeling of bolted flange connection structures are not accurate for estimating the local stress. And the evaluation of the contact state of threads and nuts in the structural response is rarely mentioned.

The bolt connection models are generally divided into four types. The first is a model that includes all the thread features, mainly used to simulate the bolt tightening process and the study of the bolt loosening mechanism caused by the contact surface slip [19]. This kind of fine hexahedral mesh model is difficult to establish. The second is a model which ignores the influence of the thread angle. In the modeling, the structure mesh can be automatically generated by sweeping. Still, the model cannot realize the phenomenon of moving along the helix because the thread angle is not considered. This model is mainly used to analyze the stress distribution of the thread. In the static analysis, the influence of the bolt thread angle can be ignored [20, 21]. The third is the I-shaped model, which is a typical simplified bolt model. This model can effectively improve the calculation efficiency. The accuracy is high in the static calculation [22]. The fourth is the model that simplifies the contact friction behavior, simplifying the bolt into beam and spring model [1], and the calculation efficiency is greatly improved. Still, the microscopic phenomenon cannot be reflected, and it is mainly suitable for the calculation of large-scale structures.

In the modeling of engineering structures, the bolt is usually simplified into an *I*-shaped structure [3, 23] by ignoring the thread details at the bolt and nut for calculation efficiency. It is not conducive to the analysis of local friction, which interferes with the response analysis of the overall structure under complex working conditions. The pressure of bolted flange connection is usually used to simulate the bolt preload in the dynamic analysis [24]. When the bolt pretightening process is ignored, the complex phenomenon in the entire connection structure cannot be restored by applying pressure alone. The complicated dynamic characteristics of bolt loosening cannot be accurately reproduced without considering the pretightening process.

One of the most attractive issues in terms of bolted joints is the loosening analysis. The findings of various experimental research on this topic have been published so far [25]. Martowicz et al. [26] discussed the effectiveness of the electromechanical impedance-based structural health monitoring system for damage diagnosis in an experiment section of a bolted pipeline. Thien et al. [27] proposed the use of macrofibre composite (MFC) transducers for structural health monitoring in pipeline systems. In the case of a plane steel frame assembled of beams, joined with bolted connections, Blachowski et al. [28] used ultrasonic approaches for structural damage detection. They simulated frame damage by removing bolts from a specific structure. Becht et al. [29] combined microphone measurements with structural data in one array for identifying loose bolts in a complex structure. Considering the tightening process of the connection, Grzejda and Parus [30] evaluated the health of a multibolted joint. In two situations, Blachowski and Gutkowski [31] used a comprehensive FEM study to investigate the connection stiffness. The first deals with all unbroken bolts, whereas the second deals with one or more broken bolts. Patil et al. [32] demonstrated the application of piezoelectric actuator to identify bolt loosening in a frame structure. Using a hybrid network of piezoelectric strain and acceleration sensors, Hasni et al. [33] developed a novel method to identify damage in steel frames in which the damage was caused by loosening the bolts and causing fractures in the structural components.

Therefore, we establish a scaled-down model of a typical bolted flange connection structure, which differs from the simplified model of the I-shaped bolt. The node coordinates are introduced into the refined finite element model of the actual connection structure, based on the hexahedral meshing of the thread structure. The model is based on a fine threaded hexahedral mesh, taking into account all the contact surfaces in the bolted connection. Considering the bolt pretightening process, we carry out the dynamic analysis of the entire bolt-flange connection structure to compare the dynamic characteristics and contact states of the integral bolted flange connection structure under different preloads, which reveals the difference between the proposed model and the traditional model. Finally, a bolt loosening detection method based on acceleration signal is provided with the corresponding simulation and experiment to verify its efficiency.

2. Finite Element Modeling of Preload Bolted Flange Connection Structure

According to the size of the rocket body, the finite element method is often used to analyze the mechanical characteristics of the structure instead of the experiment of a full-scale model. Due to the complicated characteristics of the actual interstage connection structure of the rocket, the structure is appropriately simplified, only retaining the main load-

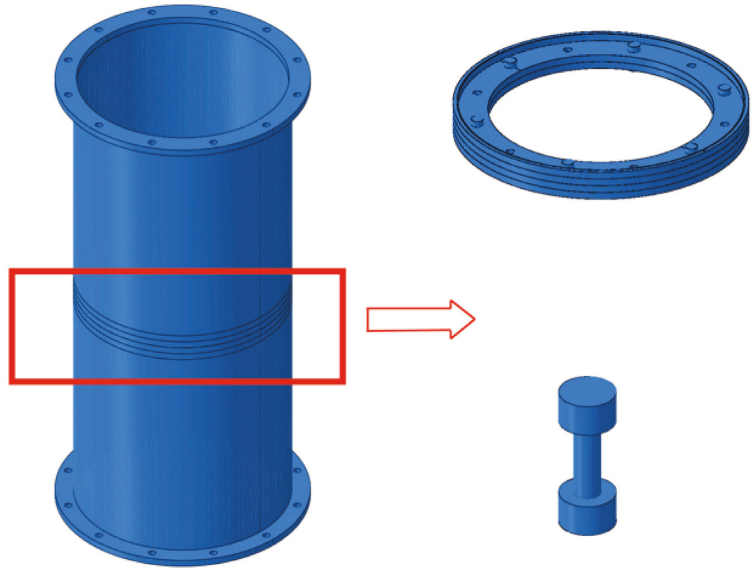

Figure 1: Simplified connection structure.

Table 1: Material properties.

Material properties	Bolt	Cylindrical section
Material	High-strength steel	Aviation aluminum alloy
Elastic modulus	210 GPa	70 GPa
Density	7850 kg/m^3	2700 kg/m^3
Poisson's ratio	0.3	0.3
Mechanical property class	12.9	

Table 2: Connection structure geometry parameters.

Geometry	Connection structure (mm)	Geometry	Bolt (mm)
Cylindrical section length	340	Head diameter	12
Wall thickness	4	Shaft diameter	5.7
Diameter	295		
Aperture	8.4		
Flange thickness	10		

bearing structure. The published work often simplifies the connection structure as a rigid spring without detailed dynamic analyses of the bolt preload. But in practical application, the loosening of bolts is an important reason for the failure of the connection structure. Therefore, it is necessary to provide a suitable finite element model for introducing the evolution of bolt preload in the dynamic analysis of the connection structure.

2.1. Traditional Modeling of the Structure with Simplified Bolt. According to the background of the relevant rocket structure, the model with a two-column structure connected by bolts of the simplified I-shape is considered, ignoring the influence of threads, as shown in Figure 1. The model parameters are shown in Tables 1 and 2. The finite element model is established by ABAQUS software with the simplified thread of the bolt in which the bolt and nut are simplified into one. The preload is applied in the form of a bolt load in the ABAQUS Load Manager which uses surface pressure to simulate bolt preload in the simplified model. For the calculation efficiency and accuracy, the C3D8R hexahedral mesh is adopted, which is divided along the axial direction. All contact surfaces in the model are set to be "hard contact" in ABAQUS, which means the augmented Lagrangian technique and the penalty approach are applied to solve the normal and tangential contact problem. The coefficient of friction is set to 0.2 in the contact surface between the bolt and the flange. The friction formula adopts the penalty function friction formula. The structure is fixed at the bottom.

In the static calculation, the preload is applied before the load is applied. The top surface is coupled and restrained at the center point, and concentrated forces of 20000 N are applied at the center point as a static load to simulate the tensile and compression experiments of the overall

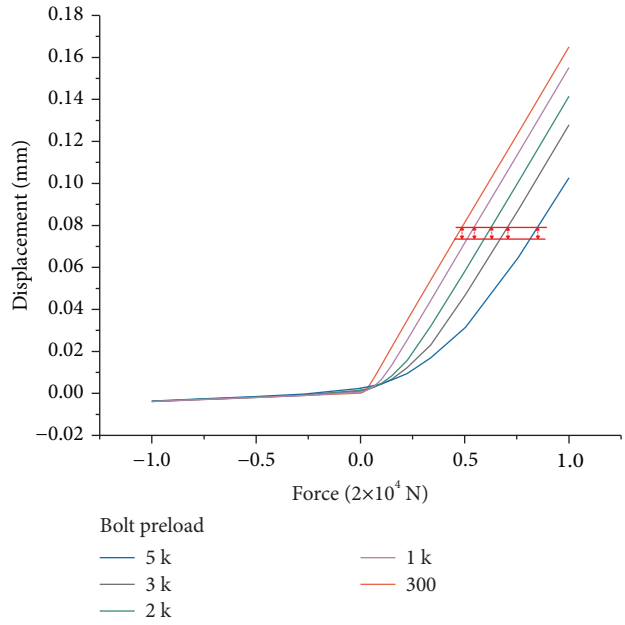

Figure 2: Force-displacement curves with different preload force.

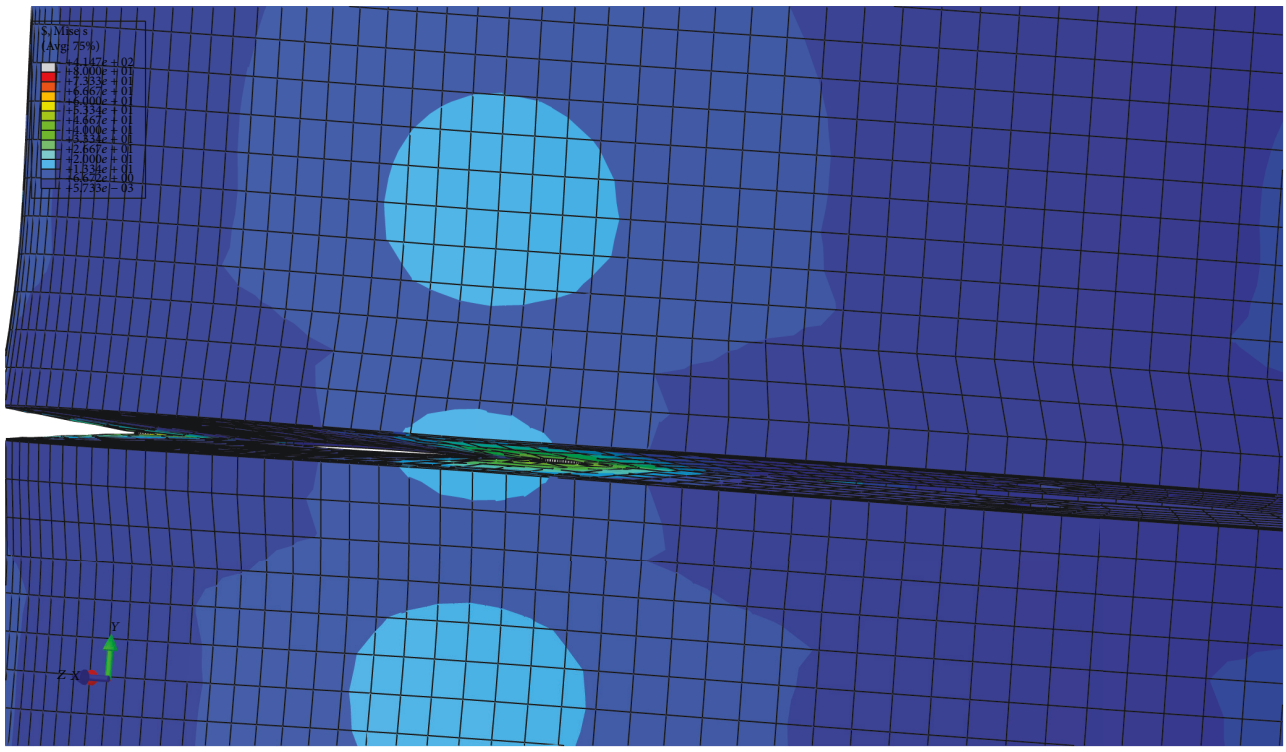

Figure 3: Partial stretch separation.

structure. Through the static analysis, the displacement and force curves of the connected structures with different preload forces of the bolts can be found obviously nonlinear, as shown in Figure 2. The increasing preload force leads to more rigidity if a tensile load is applied. As the tensile load increases to a certain extent, the slope of the curve does not change. When the tensile force exceeds 10000 N, the force-displacement curves under different preloads are close to a parallel state, and the displacement increase caused by the increase of the tensile force is almost equal. At this time, the flange surface is partially separated in Figure 3. The bolt preload has little effect on the rigidity of the connection structure as the tensile stiffness remains constant. When a compressive load is applied, the value of the preload has little effect on the stiffness curve, because it is the cylindrical shell rather than the bolt that bears the compressive load.

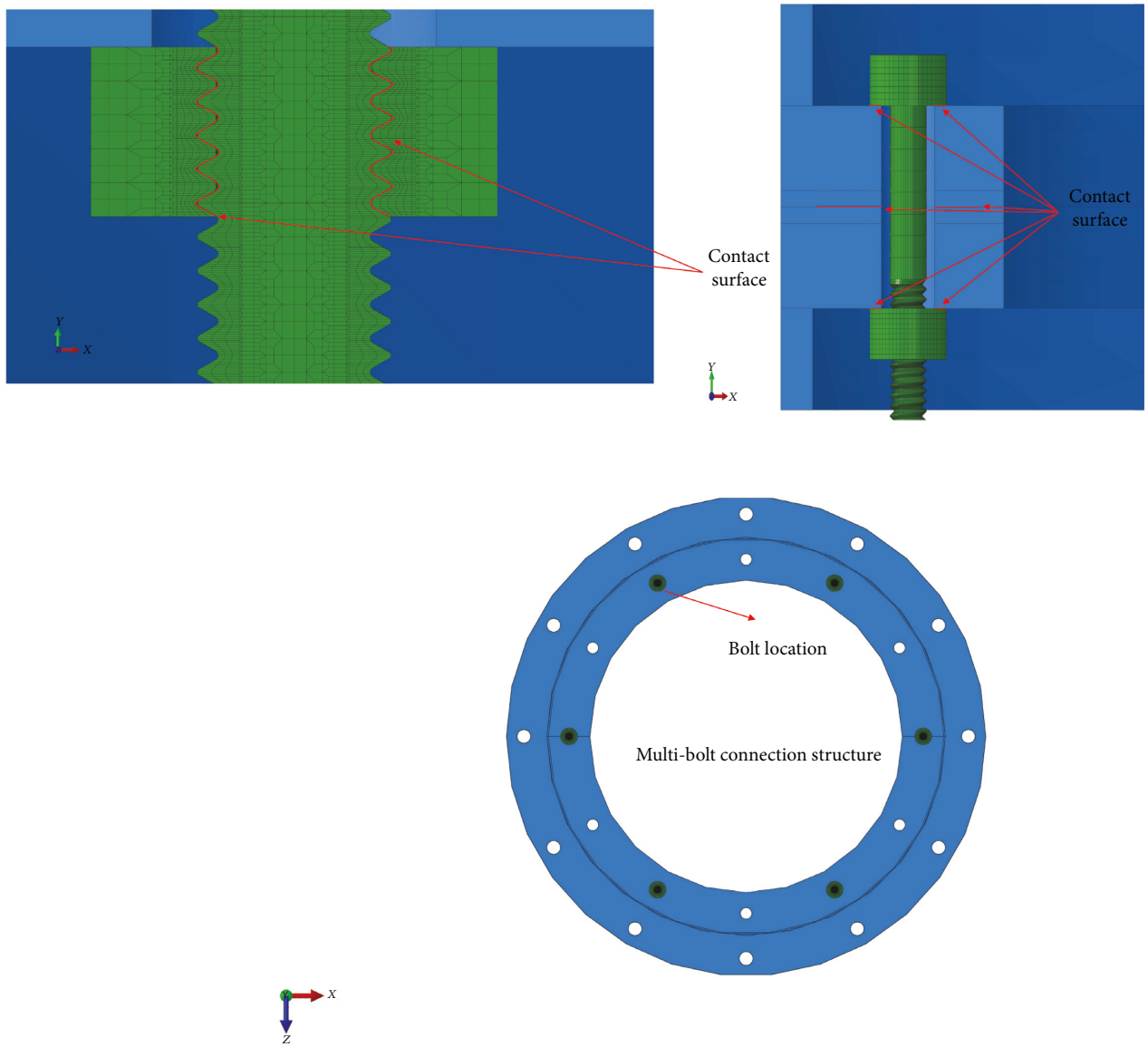

Figure 4: Connection structure contact surface.

So, the effect of bolt preload on the mechanical properties of the connection structure cannot be ignored. We present a new model of the connection structure instead of the traditional simplified model in the following part.

2.2. Specified Modeling of the Structure for Simulation of Tightening Process. When the bolt is simplified to an I-shaped structure in the finite element model for dynamic analysis of the connection structure, the calculation is more efficient. Still, the influence of the thread cannot be considered. That means the local stress and contact state cannot be effectively simulated and predicted. So, we introduce the detailed thread bolts into modeling the integral bolted flange connection structure extending from Chen et al. and Li et al.'s work [34, 35]. They introduced fine thread contact using rigid constraints on the joint surface of a single bolt-connected block structure. We extend it to the multibolt connection structure as shown in Figures 4 and 5, in which each contact area between the bolt, the nut, and the flange is elastic. Contact interactions have been set between all sliding surfaces, including the interfaces between the threads, the bolt underhead surface, the upper part surface, the nut surface, and the lower part surface. Then the response with varying local contact of the connecting structure can be analyzed under external load.

The shape of the thread is inherently similar at any cross section along the bolt axis, according to the geometry features given in Figure 6. Just rotate the axis at a given angle to produce a different cross section. The pitch is equal to the outside contour line of the cross section. The thread root radius and the cross section shape along the bolt axis are shown in Figure 6.

The formula for fine hexahedral mesh generation of the thread cross section profile [34]:

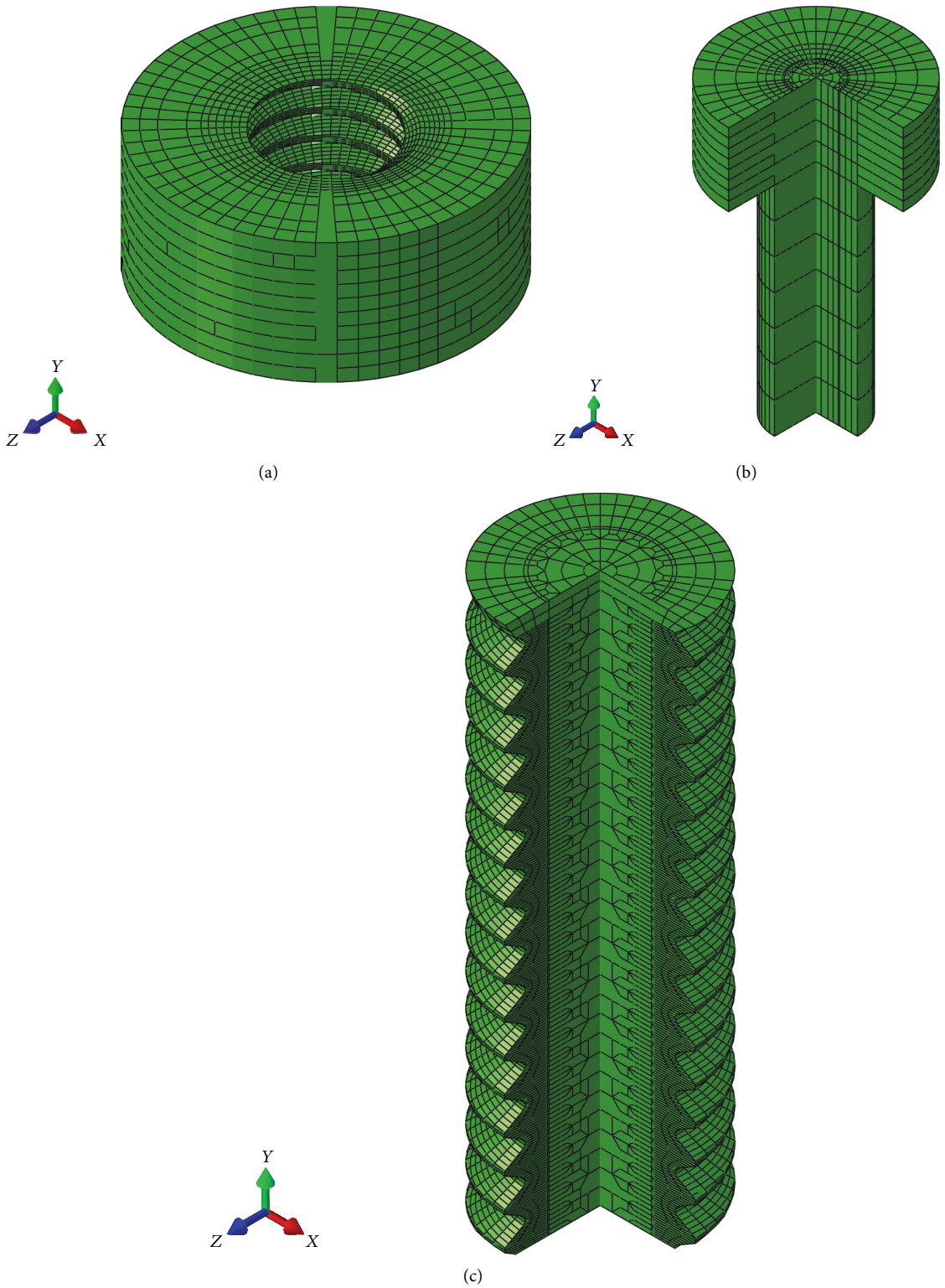

Figure 5: Hexahedral model. (a) Nut mesh. (b) The bolt head mesh. (c) The screw thread mesh.

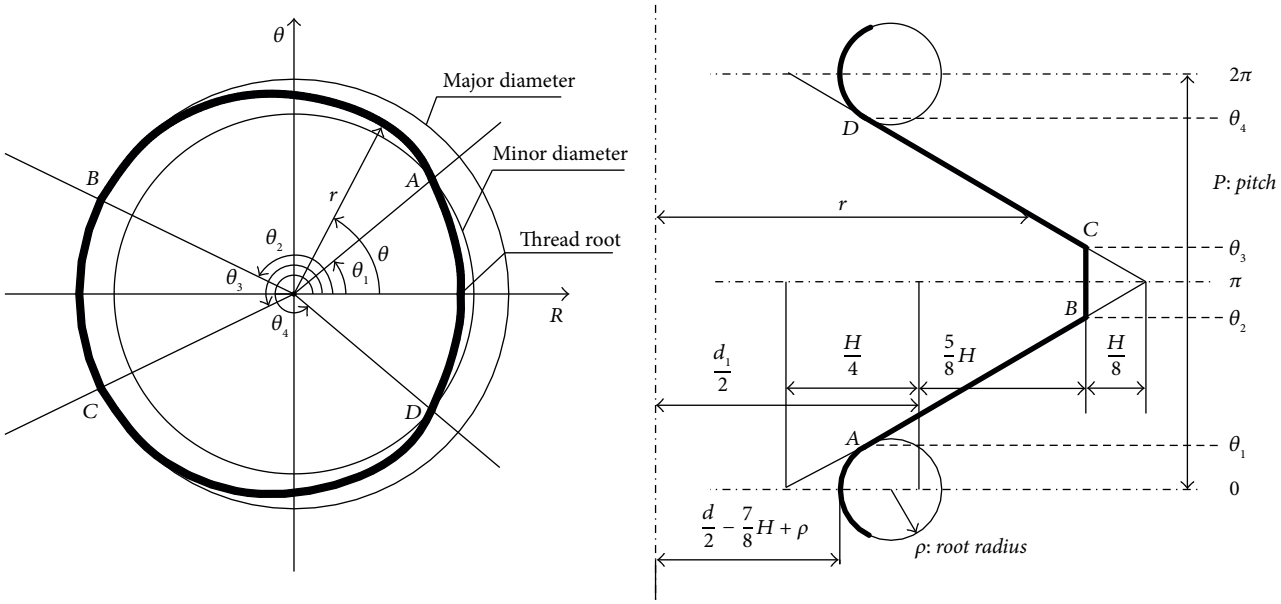

Figure 6: The section profile of the external thread and along the bolt axis [34].

$$r(\theta,z)=\begin{cases}\phi=\theta+\varphi=\theta+\dfrac{2\pi}{P}z,\\ \dfrac{d}{2}-\dfrac{7}{8}H+2\rho-\sqrt{\rho^2-\dfrac{P^2}{4\pi^2}\theta^2}, \quad (0\le\phi\le\theta_1),\\ \dfrac{H}{\pi}\theta+\dfrac{d}{2}-\dfrac{7}{8}H, \quad (\theta_1\le\phi\le\theta_2),\\ \dfrac{d}{2}, \quad (\theta_2\le\phi\le\theta_3),\\ \dfrac{H}{\pi}(2\pi-\theta)+\dfrac{d}{2}-\dfrac{7}{8}H, \quad (\theta_3\le\phi\le\theta_4),\\ \dfrac{d}{2}-\dfrac{7}{8}H+2\rho-\sqrt{\rho^2-\dfrac{P^2}{4\pi^2}(2\pi-\theta)^2}, \quad (\theta_4\le\phi\le2\pi),\end{cases}$$

$$\theta_1=\frac{\sqrt{3}\pi\rho}{P},$$

$$\theta_2=\frac{7\pi}{8},$$

$$\theta_3=\frac{9\pi}{8},$$

$$\theta_4=2\pi-\theta_1\rho\le\frac{\sqrt{3}P}{12},$$

$$H=\frac{\sqrt{3}}{2}P. \tag{1}$$

In this formula, the thread pitch and nominal diameter are denoted by P and d. The thread's root radius is ρ. The shape of another cross section, which is a distance z off the datum plane, is identical to the datum one.

For simulating the bolt tightening process in the fine thread model, a cylindrical coordinate system is established, and a tangential displacement is applied to the outer surface of the nut to replace the actual torque. The entire process of loading is divided into three parts. Firstly, the bolt head is fixed, and the outer node of the nut applies tangential displacement. Secondly, the tangential displacement is maintained for a period of time based on the previous step. Finally, the bolt head restraint is released. During the loading process, the preload and the tangential displacement increase together. When the constraint is released, the preload temporarily decreases. This method simulates the loading process practically.

2.2.1. Static analysis. Consider the connection structure with 6 bolts under stable preload. Simulating the bolt stress distribution, we have the tightening torque:

$$T_f=KF_fd, \tag{2}$$

where F_f is the bolt preload, d is the bolt's nominal diameter, and K is the torque coefficient [36]. The value of K is 0.253 in this paper. This value results from the calibration of the finite element model and conforms to the GB/T 16823.2 [36]. This section uses the same contact setup as above and applies tangential displacements of 2 mm to the bolts on the detail model and performs finite element calculations to observe the stress characteristics of the bolts after the preload process. After preload process, the preload of bolt is about 5000 N. The stress distribution of the new bolt model is shown in Figure 7 compared with that of the traditional I-shaped simplified model. The new bolt model and the *I*-shaped bolt have different stress distributions after the preload process. The *I*-shape model has a more uniform and idealistic stress distribution, while the detail model shows a gradient with the maximum stress on the threads, which is

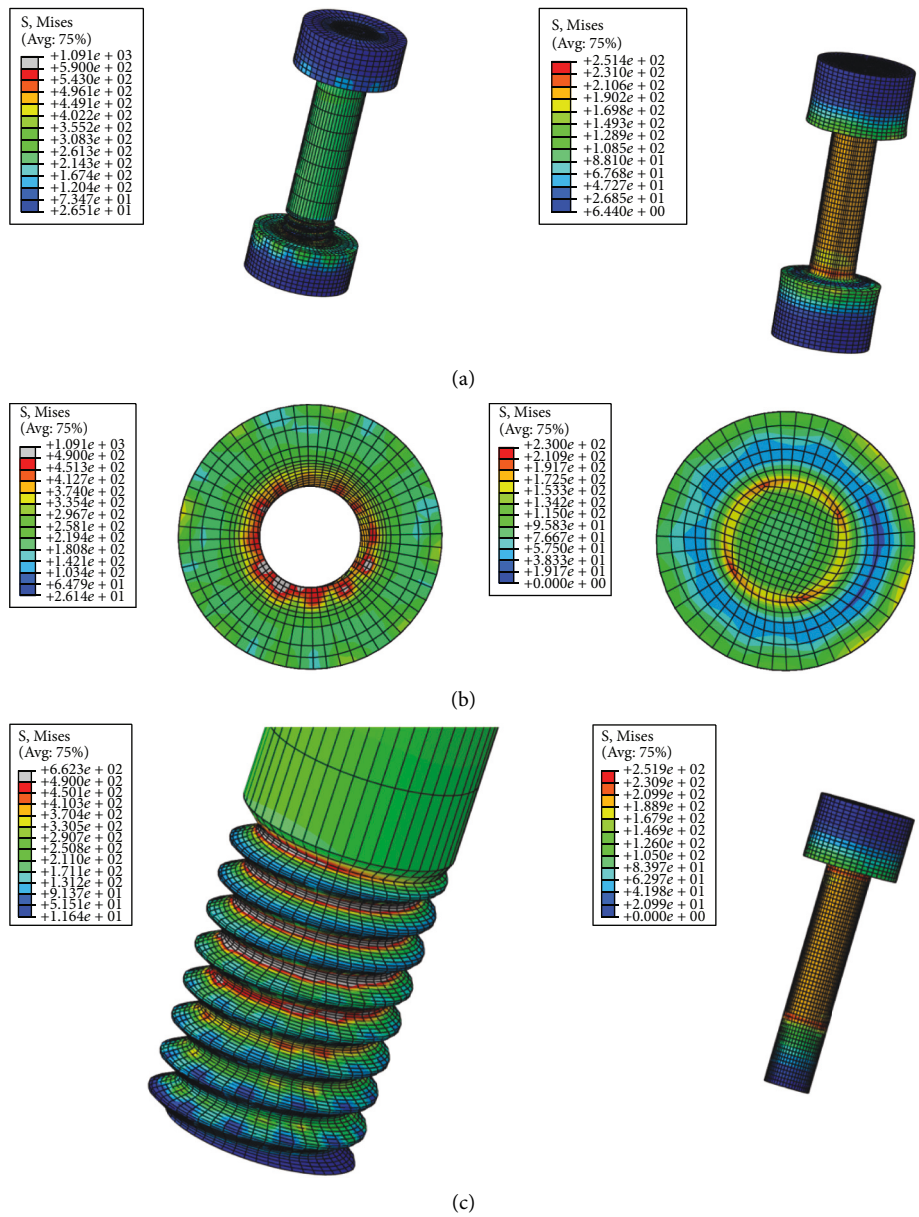

Figure 7: Stress comparison of two different preloaded models. (a) Overall bolt stress comparison (side view). (b) 7-nut stress comparison (vertical view). (c) Screw stress comparison.

closer to the working condition of thread wear. The threads wear to a certain extent after the bolts are preloaded and disassembled in actual working conditions. This wear is clearly caused by exposure to excessive stresses, which cannot be considered in conventional simplified models. Hence, the model used in this paper is more effective for estimating local contact stresses.

In the nut contact part, the contact area of the traditional *I*-shape modeling is relatively uniform, and the stress value is obviously smaller. However, the stress distribution of the new model considering the screw thread is more accurate and closer to the reality, showing a nonuniform distribution, and the maximum stress appears at the edge of the thread tooth. This cannot be considered in the traditional I-shape model.

Traditional *I*-shape bolt modeling underestimated the thread stress at the contact between the nut and the thread in Figures 8 and 9. The detailed model used in this paper can effectively calculate the stress of the thread during the loading process, which is beneficial to analyze the bearing capacity of the bolted flange connection structure, and can accurately judge the occurrence of the invalidation.

Through comparison, it is found that the maximum stress of the traditional model occurs at the screw, while the maximum stress of the fine thread model occurs at the thread teeth. It gradually decreases from the outside to the inside, and the analysis accuracy is greatly improved. In terms of overall stress, the maximum stress of the traditional model is 251.9 MPa, which is an order of magnitude lower than the 1091 MPa of the fine model. The traditional

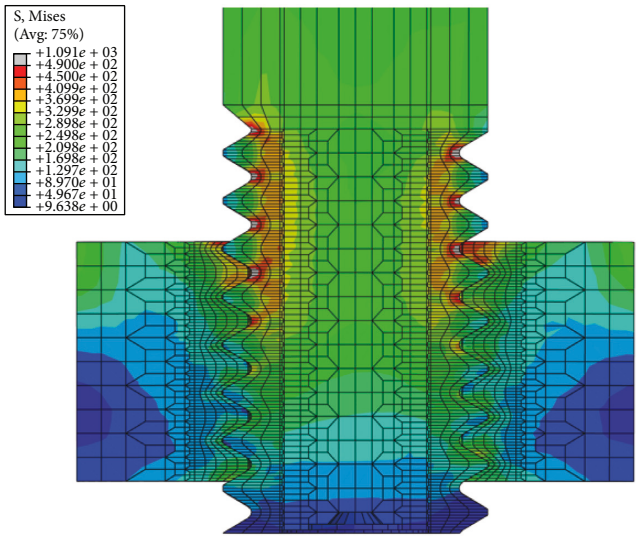

Figure 8: Detailed bolt section stress.

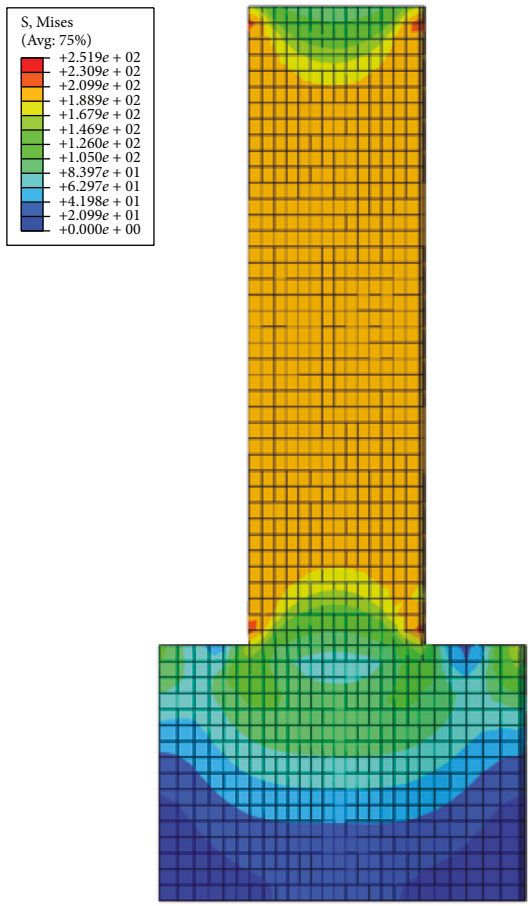

Figure 9: Simplified bolt section stress (after preload process).

modeling method underestimates the local stress of the bolt joint. After preload process, the stress predictions of the two modeling methods are significantly different, so this paper will continue to compare the dynamic characteristics of the two modeling methods in the following text.

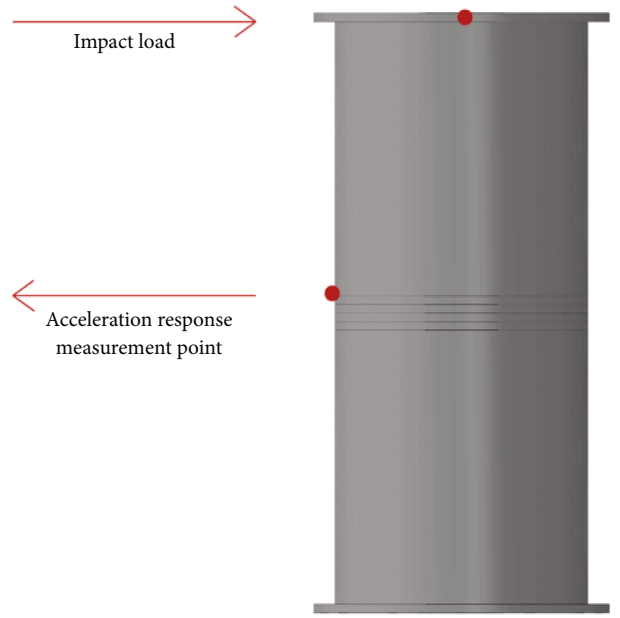

Figure 10: Schematic diagram of the calculation model.

2.2.2. Dynamic analysis. When the connection structure with 6 bolts has completed the pretightening process, an impact load of 1500 N is applied to the top of the connection structure in Figure 10, and the impact time is 0.002 s. The contact parameter settings remain the same as in the static calculations above. The calculation is performed in ABAQUS using implicit dynamics calculation steps, and the observation point is located at a distance of 20 mm from the connection surface. The results of the calculations are compared with the simplified model of the *I*-shape bolted flange structure.

The acceleration and amplitude of the two modeling techniques in the X and Y directions are similar under a 1.5 kN impact load, but the amplitude attenuation rate is different in Figures 11 and 12. According to this article, traditional modeling methods are still useful in overall response analysis, although there are some changes in frequency components.

The FFT transformation of the acceleration signal reveals that the two modeling approaches' first-order frequency and amplitude are almost identical in Figure 13, and the bending mode fitting is identical. However, minor changes are between the refined and simplified models in the intermediate and high-frequency regions. The fine model's frequency is slightly lower than the simplified model's, but its amplitude is considerably higher. Longitudinal deformation modes dominate these middle- and high-frequency modes. The longitudinal response is influenced more by the diverse pretightening forms and simplified ways of the bolt and flange connection structure in the finite element analysis.

Comparing the two modeling methods, there is almost no difference in the x-direction horizontal projection friction of the overall connection surface. Still, the simplified model is overestimated for the friction at the nut, which is not conducive to the safety margin analysis in Figure 14.

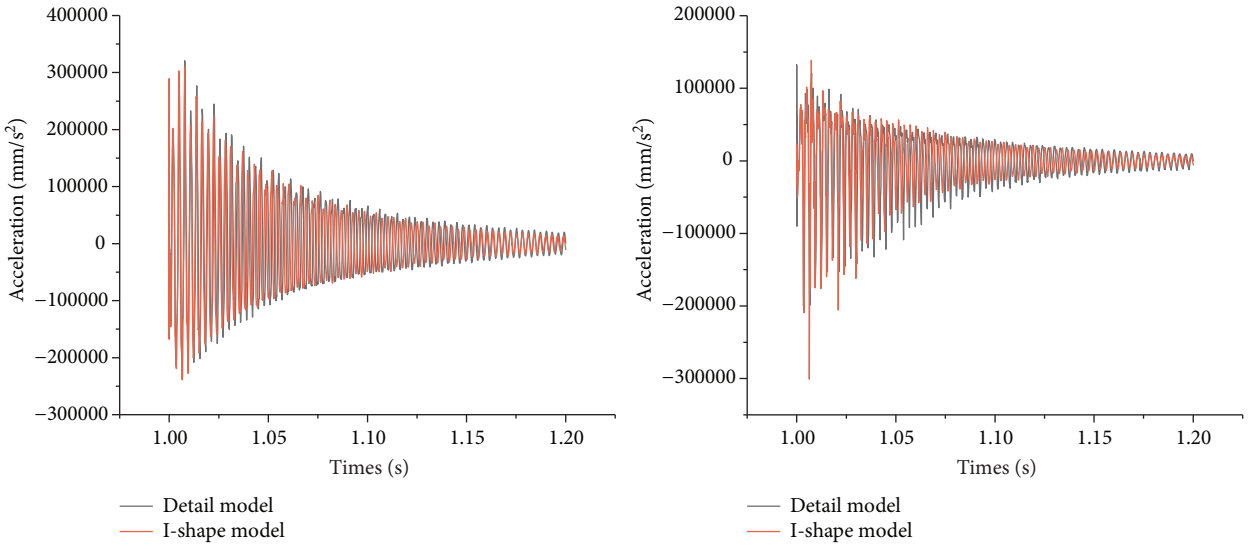

Figure 11: X and Y direction acceleration response (at the outer wall of the flange under 1.5 kN impact load on the top).

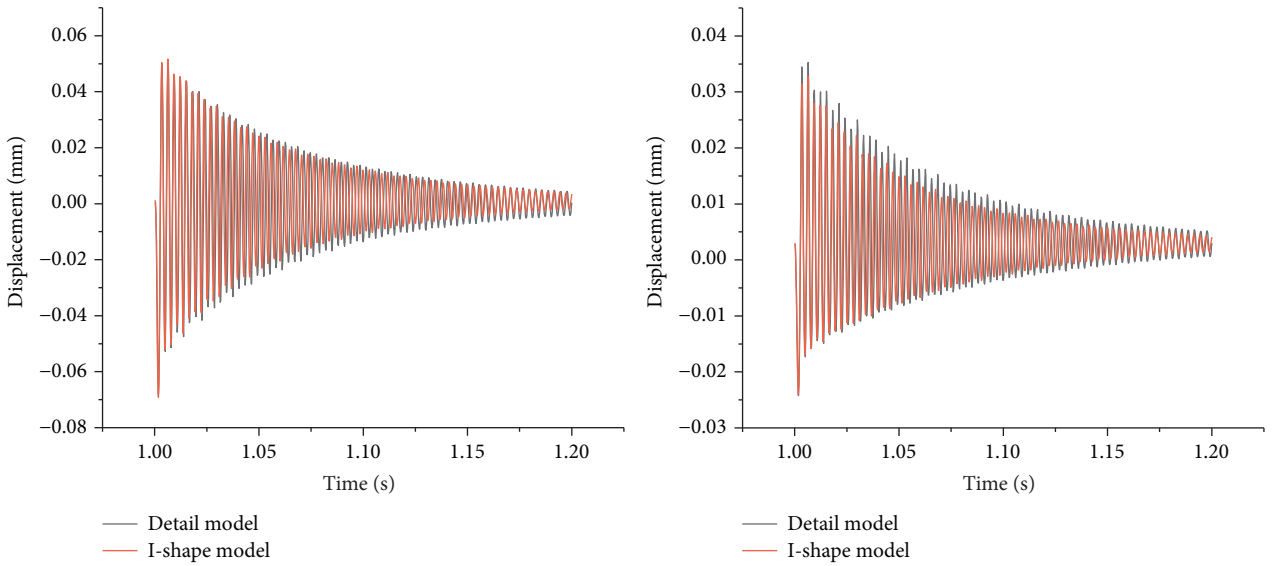

Figure 12: X and Y direction displacement response of the connection structure under 1500 N impact load on the top.

According to the analysis, this is because the traditional I-shaped modeling does not consider thread friction, so it can only compensate for the force balance on the nut. But in fact this is not accurate, which will increase the wear of the nut without considering the friction damage to the thread. However, in engineering practice, thread damage is more common. The bolts will be loose due to the damage, putting the entire connection structure at risk. As a result, the connection structure with loosening will be investigated based on this fine modeling method in the following.

2.2.3. Loosening analysis. In the bolted flange connection structure, bolt loosening is often an important reason and performance of structural failure. In the case of loose bolts, the dynamic characteristics of the bolted flange connection structure will undergo special changes. Therefore, based on considering the bolt pretightening process and the fine bolt modeling, this paper conducts a dynamic analysis of the bolted flange connection structure under the impact load. An impact load of the same magnitude on the top of the thin-walled connection structure is applied. The dynamic response characteristics of the connection structure are observed before and after the bolts go loose. It is worth noting that achieving the impact of vibration using implicit dynamic calculation is extremely challenging. As a result, to simulate loosening situations, this article uses an artificial setup of low preload, which helps increase computation efficiency. The type and amplitude of the impact load are the same as above.

The loose bolt will change the contact state of the connecting surface. The blue area in Figure 15 represents the uncontacted area, the red area represents the sticking area, and the green area represents the microslip area. When

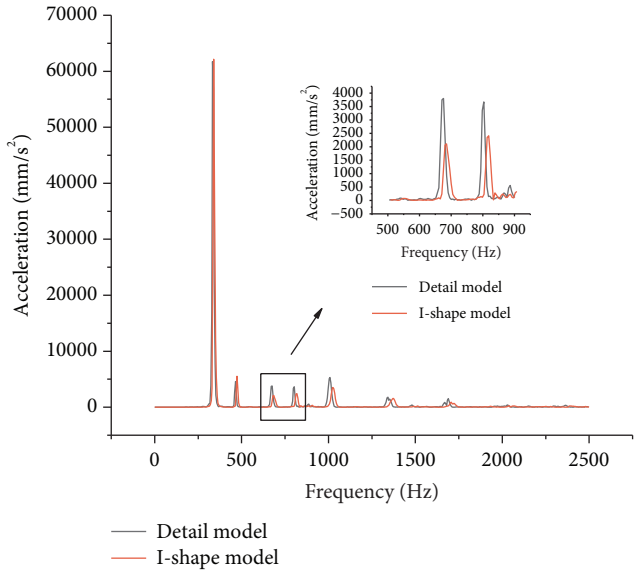

Figure 13: Amplitude-frequency curve.

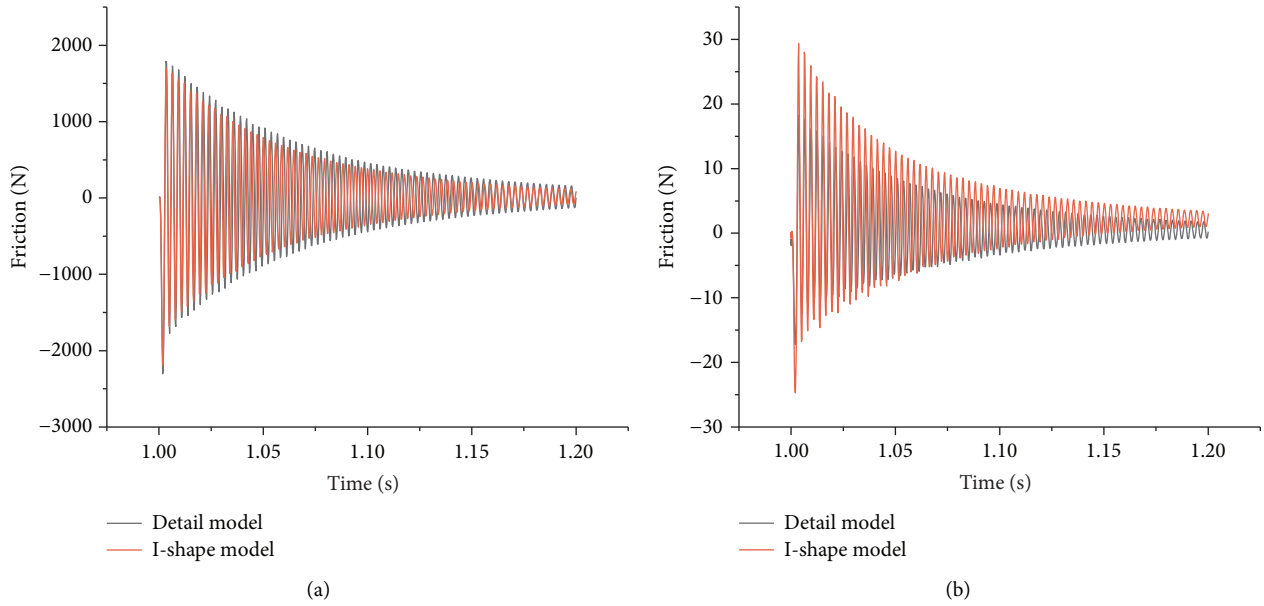

Figure 14: x-direction horizontal projection friction. (a) Flange surface. (b) Nut surface.

loosening occurs, the area of the sticking area between the flanges near the loose bolt area will increase, causing repeated friction. The bolt area on the no loosening side is almost unaffected, so the adverse effects caused by bolt loosening mainly occur in the outer edge area of the flange where the loosening occurs. Repeated sticking area and friction will cause local stiffness loss and may even lead to failure of the connection structure. This explains the mechanism of the abnormal dynamic response of the connection structure when the bolt is loose.

Through the implicit dynamic calculation of the impact load applied to the bolted flange connection structure containing a loose bolt, it can be found that, during the entire vibration process, the sticking area near the loosening of the flange connection structure containing loose bolts increases significantly in Figure 16. A certain degree of the slipping area appears. These are the main structural features when loosening occurs.

Without loosening, the sticking area of thread contact is more continuous at the upper and lower interfaces, while the middle part is slightly discontinuous. As the loosening occurs, the sticking area of the upper and lower sections of the thread becomes discrete and the area becomes smaller in Figures 17 and 18. This interval sticking zone reduces the

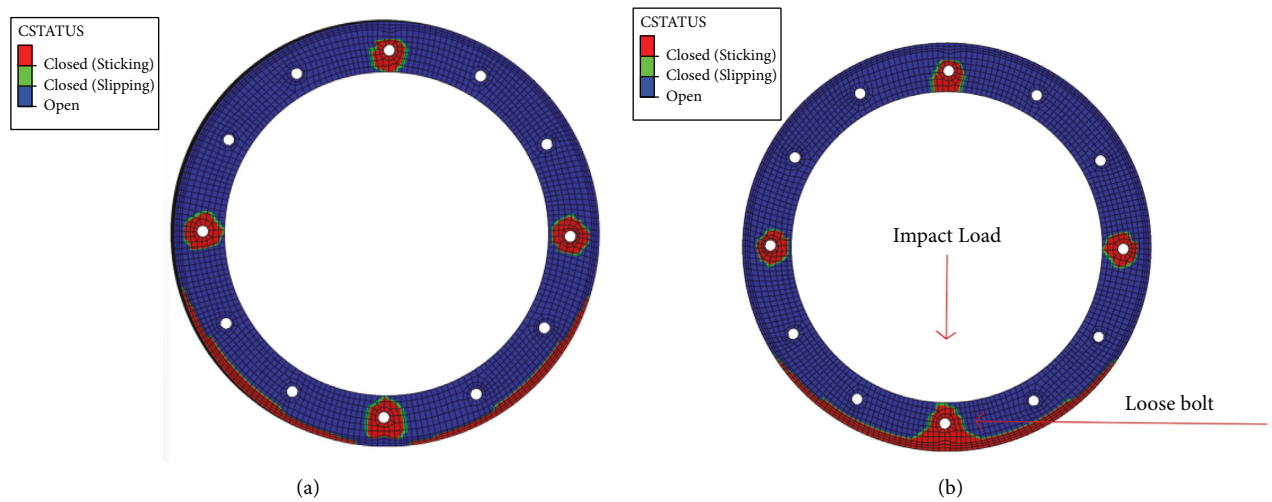

Figure 15: Connection surface contact state (4 bolts in the structure under 1500 N impact load on the top). (a) No loosening with 5000 N bolt preload. (b) Loosening to 300 N bolt preload.

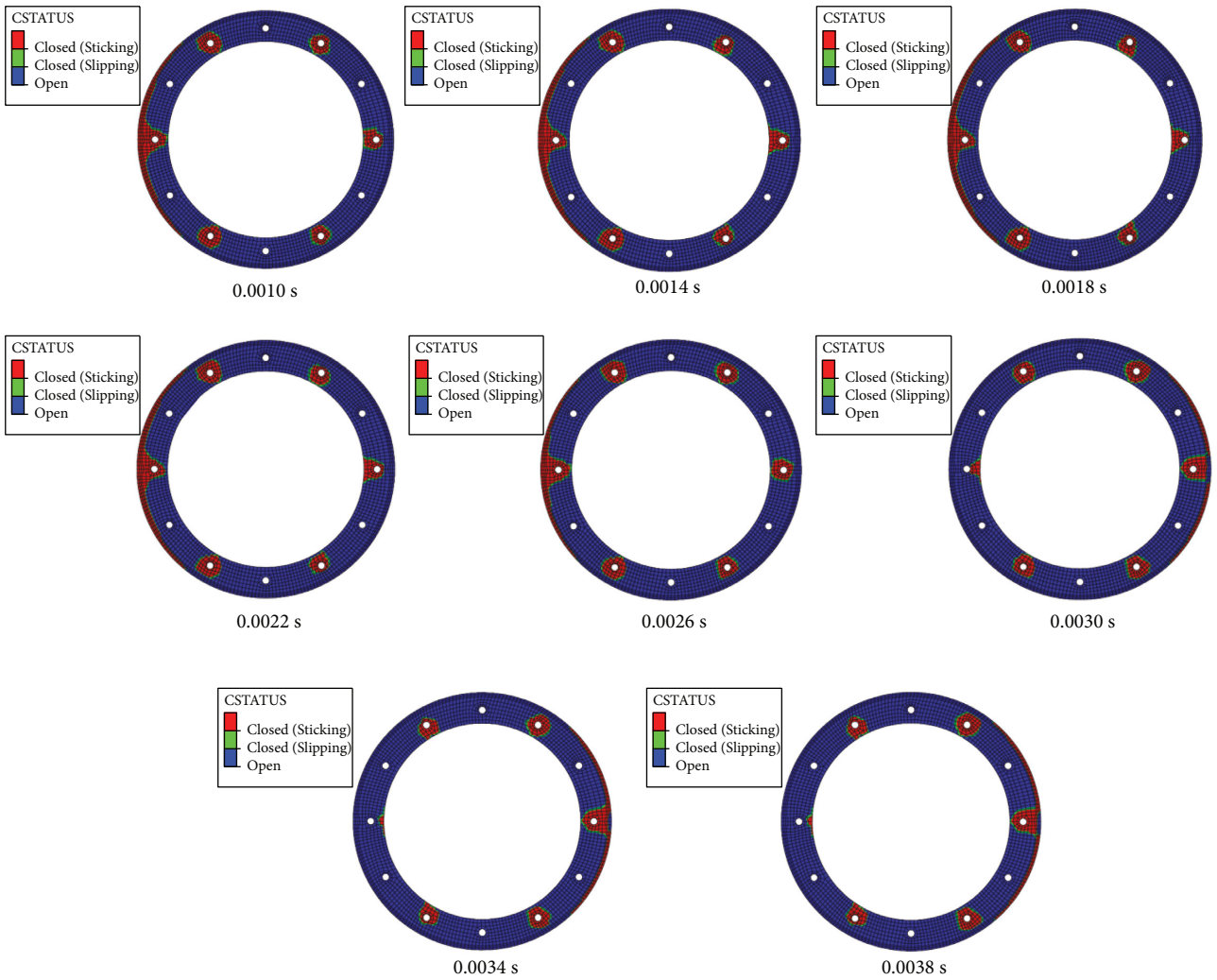

Figure 16: Time-varying diagram of the contact state of the connecting surface during the impact (6 bolts' flange structure with one bolt loosened to 300 N under 1.5 kN impact load on the top).

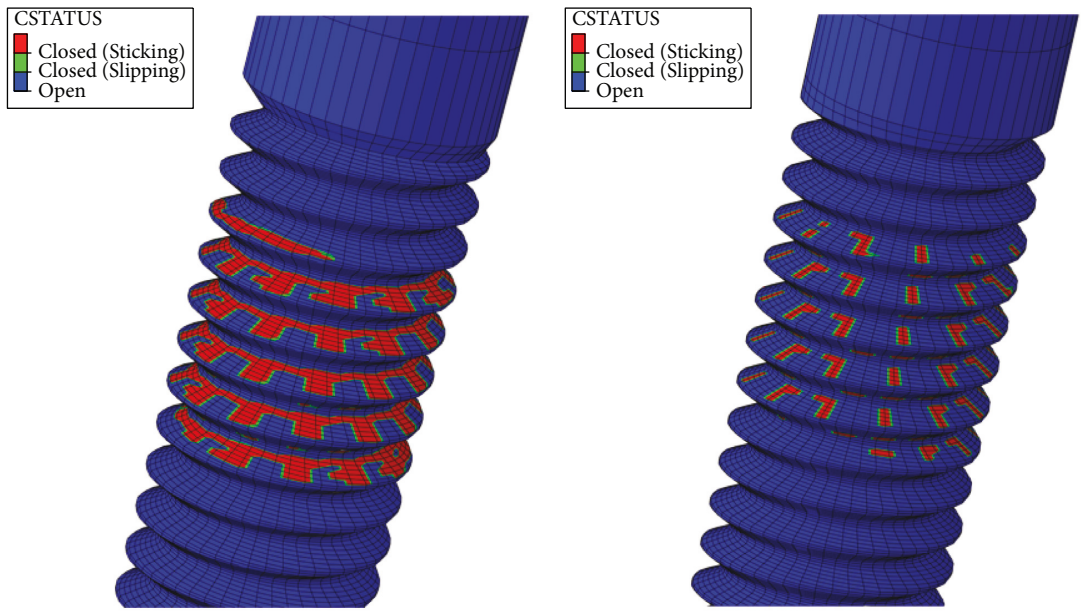

Figure 17: Thread contact state (six bolts' flange structure under 1.5 kN impact load on the top). (a) No loosening with 5000 N bolt preload. (b) Loosening to 300 N bolt preload.

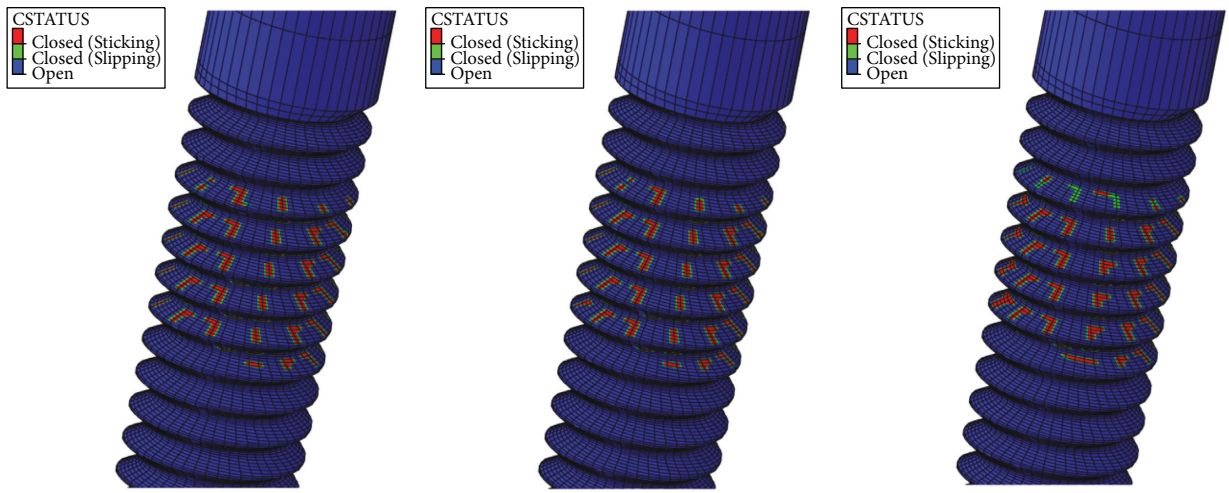

Figure 18: Time-varying graph of thread contact state under impact load (the loose bolt to 300 N preload under 1.5 kN impact load on the top).

torsion resistance of the bolt, and the local slippage occurs, and the cumulative slippage will become an unstable factor for the entire connection structure.

Since the entire connecting surface is an elastic body, the friction at the joint surface can be analyzed. It can be found that when the loosening occurs, under the impact load of 1500 N, the instantaneous friction peak value of the overall connection surface does not change significantly. However, as the subsequent vibration attenuates, the frictional force of the loosening connection surface attenuates significantly faster, and the subsequent amplitude is smaller in Figure 19.

When loosening occurs, the friction force at the nut increases slightly, and the attenuation speed is faster, consistent with the change law of the overall friction force of the connecting surface. However, the friction at the thread is quite different. When loosening occurs, the friction peak at the thread will change drastically, the degree of fluctuation will be greater, and the decay rate will be faster. This can also cause the bolt connection to be unstable, leading to damage to the thread.

The stress on the loose bolt is lower than the stress on the no-loose bolt during the impact, and the stress distribution is

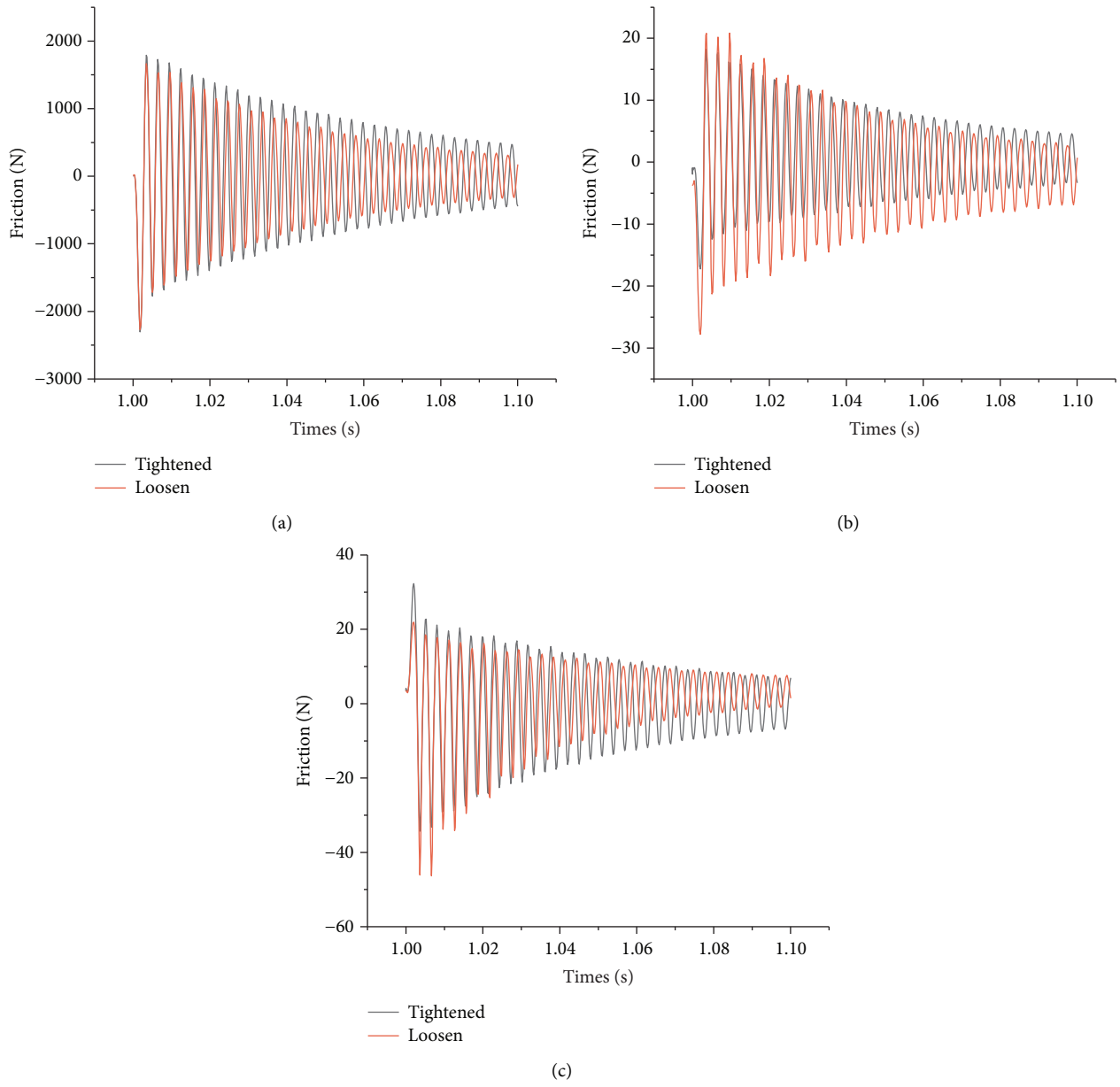

Figure 19: x-direction horizontal projection bolt local friction (under 1.5 kN impact load on the top). (a) Flange surface. (b) Nut surface. (c) Thread surface.

uneven. At a certain point, the bolt on the loose side will alternately appear with the greatest stress on both sides in Figure 20. The total highest stress of the loose bolt arises on the side away from the center of the joint surface and at the thread during the entire vibration process.

The FFT transformed acceleration signals of the connection structure with a loose bolt or without any loose bolt are derived separately from the dynamic calculations of the impact load model using the fine model presented in Figures 21–23. Although the data demonstrate a difference in the amplitude-frequency curves between loosening and nonloosening, they are not intuitive and require the experience of enough technicians to determine. Engineers would like to develop a more user-friendly and convenient monitoring approach.

Because the implicit dynamics calculation indicates that a flange connection structure with loose bolts will have a distinct response state, the following text will attempt to develop a practical and intuitive approach for detecting loosening conditions based on these features.

3. Loosening Detection of Preload Bolted Flange Connection Structure

3.1. Loosening Detection Method. Loose bolts are extremely harmful while the connection structure is in use. The best way to spot this flaw is to use timely signal detection. However, indirect measurement is usually employed to detect loose bolts because it is sometimes not possible to put a pressure sensor in the actual connection structure. The

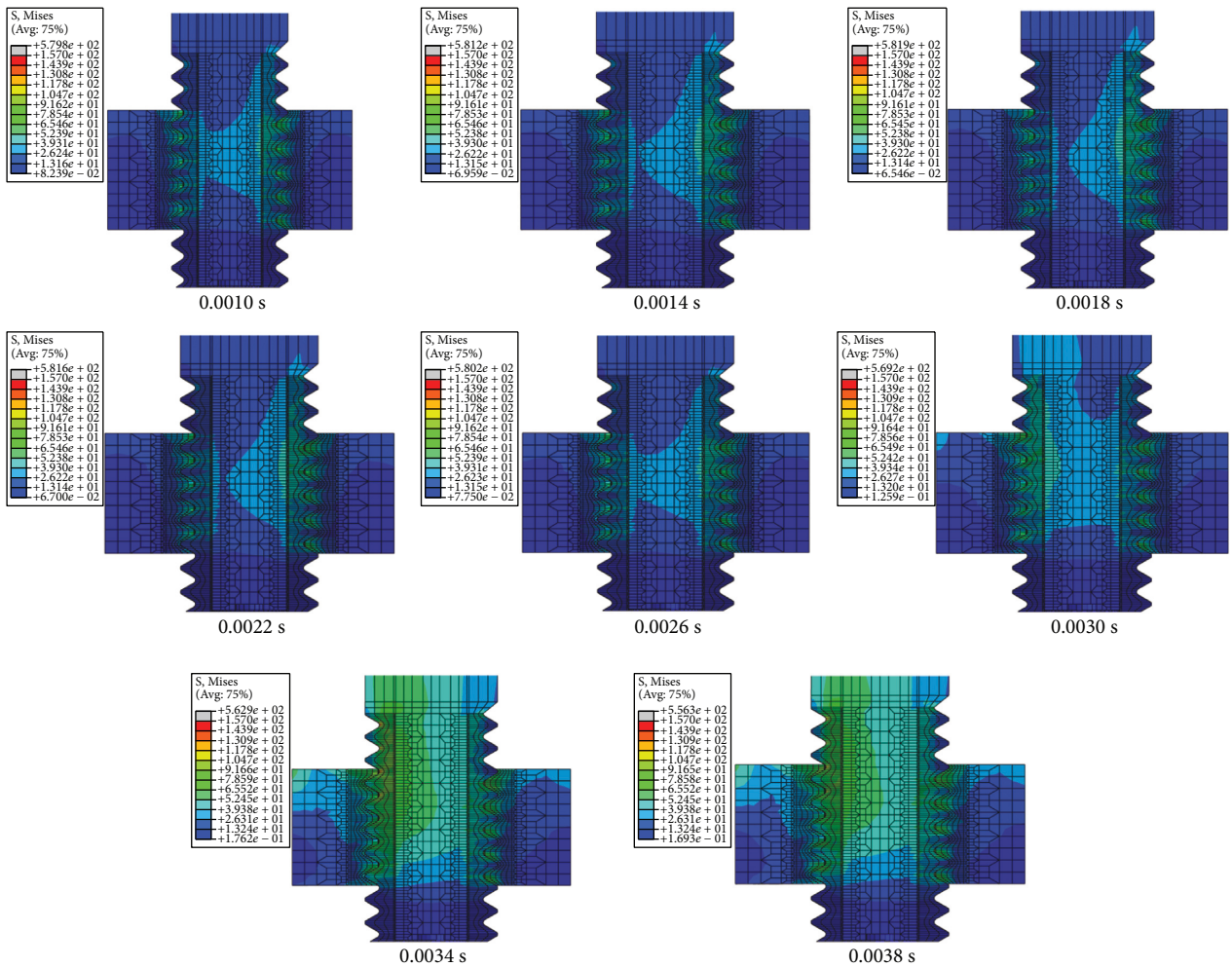

Figure 20: Time-varying graph of bolt section stress under 1.5 kN impact load (the loose bolt in six bolts' flange structure).

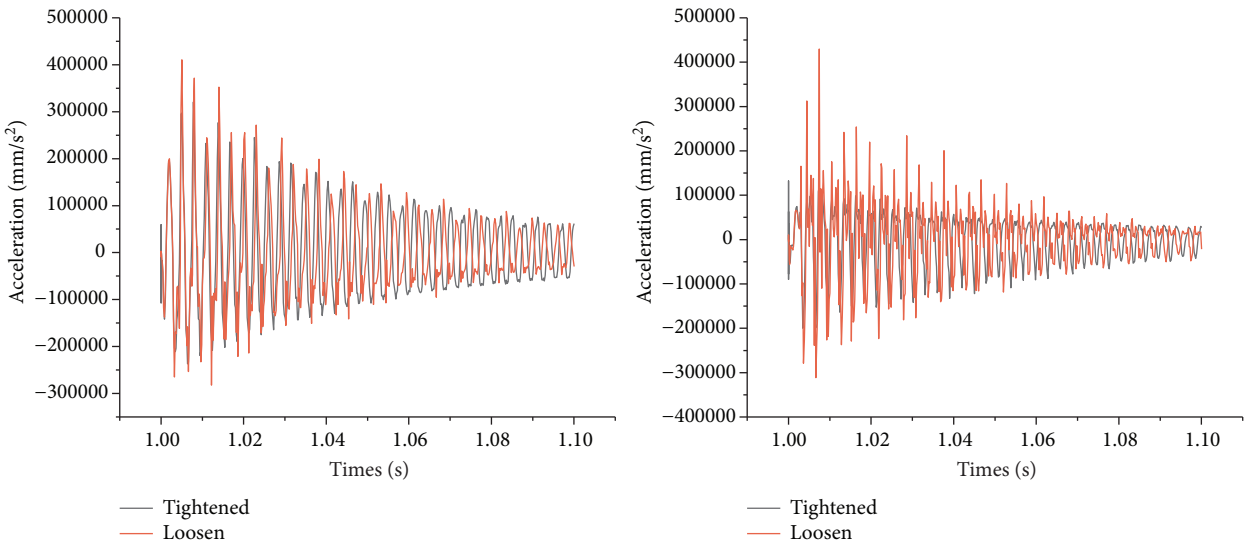

Figure 21: X and Y direction acceleration response (under 1.5 kN impact load on the top).

acceleration value is usually quite straightforward to measure in the actual structure, and an acceleration sensor can monitor it. A numerical processing approach for determining loosening based on acceleration signals is established in this study by examining the time-frequency domain results of the finite element model dynamics.

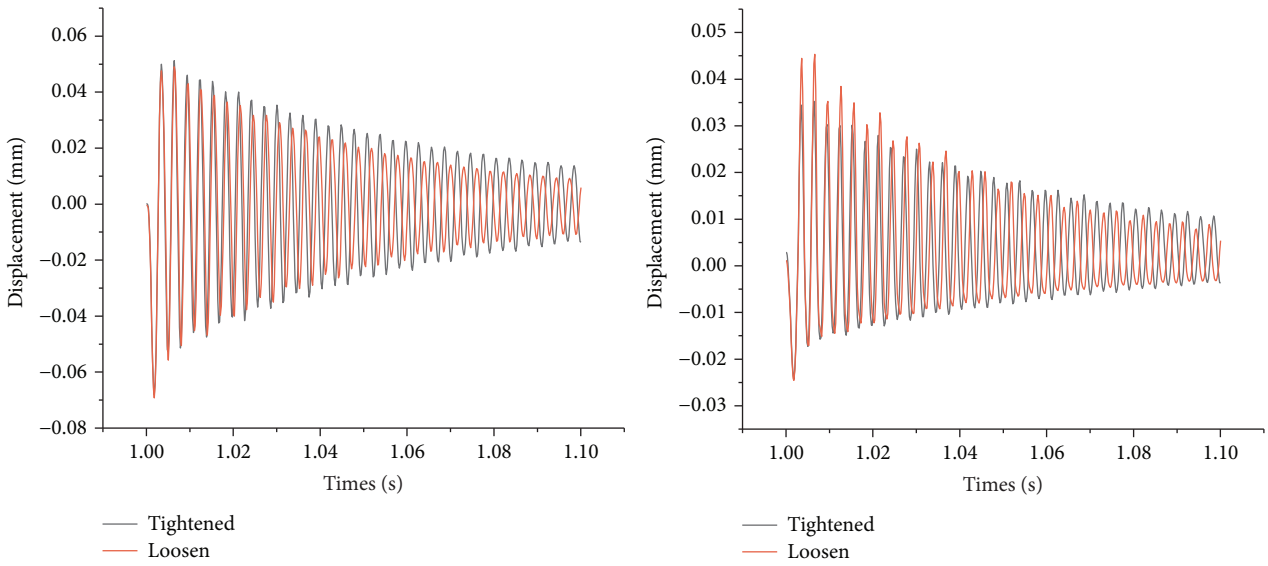

Figure 22: X and Y direction displacement response (under 1.5 kN impact load on the top).

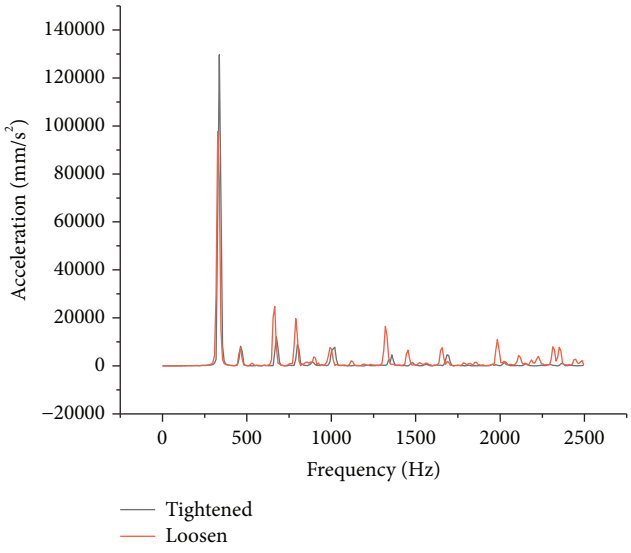

Figure 23: Amplitude-frequency curve.

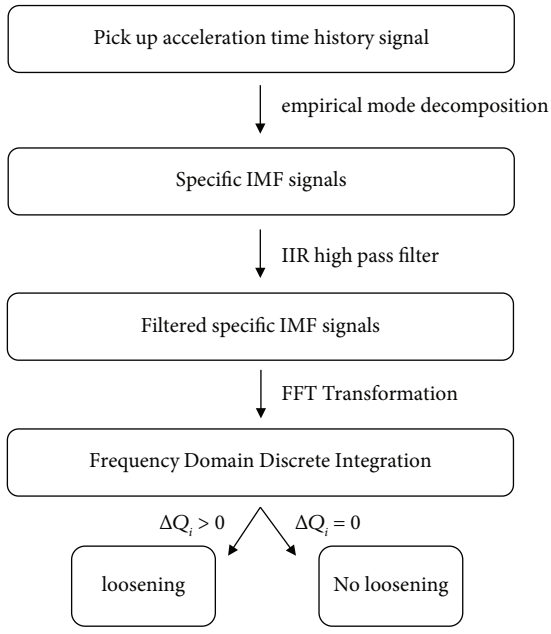

Figure 24: Loosening identification flowchart.

After bolt loosening occurs, nonlinear characteristics will enhance at the dynamic response level, and nonlinear states will appear in the time and frequency domains. In the study of Luan et al. [2], due to the nonlinear tension and compression stiffness of the connection surface, the flange connection structure itself has a nonlinear characteristic transverse and longitudinal coupling dynamic analysis, so that the characteristic signal of bolt loosening is covered to a certain extent. This is not conducive to analysis, so the signal needs to be processed. Huang et al. proposed EMD (empirical mode decomposition) to perform adaptive signal analysis in the time and frequency domain [37]. This algorithm has received extensive attention and applications in structural monitoring. Generally, high-frequency indicators are more sensitive to damage. When the time-domain signal is used directly, the frequency components of the low frequency band often account for a large proportion, which is not conducive to the analysis of bolt loosening. Therefore, it is first necessary to perform EMD decomposition of the time-domain signal to separate the data information of the characteristic frequency band. The EMD algorithm decomposes the fluctuations or trends of the original signal on different scales in the time domain of the signal step by step and generates a series of data sequences that retain local feature information, that is, intrinsic mode function (IMF). The original signal can be expressed as the sum of n-th order IMF components and residuals. The principle formula of EMD is as follows:

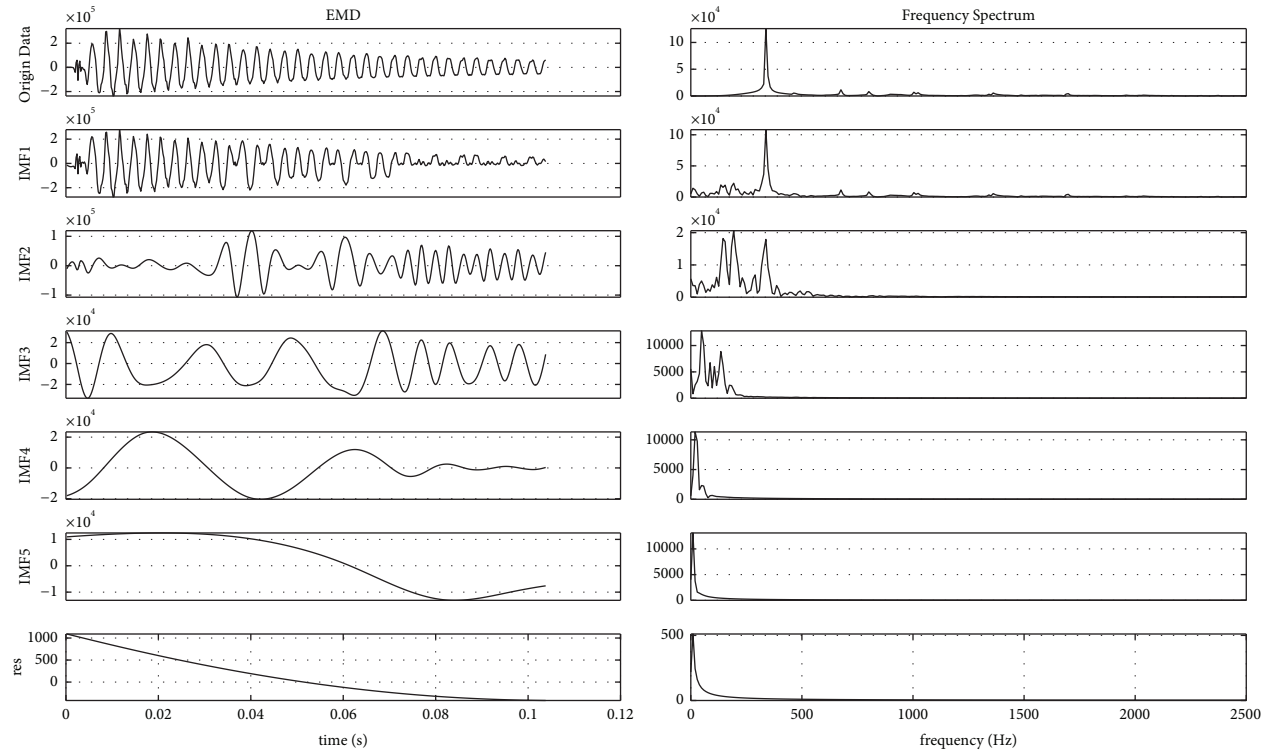

(a)

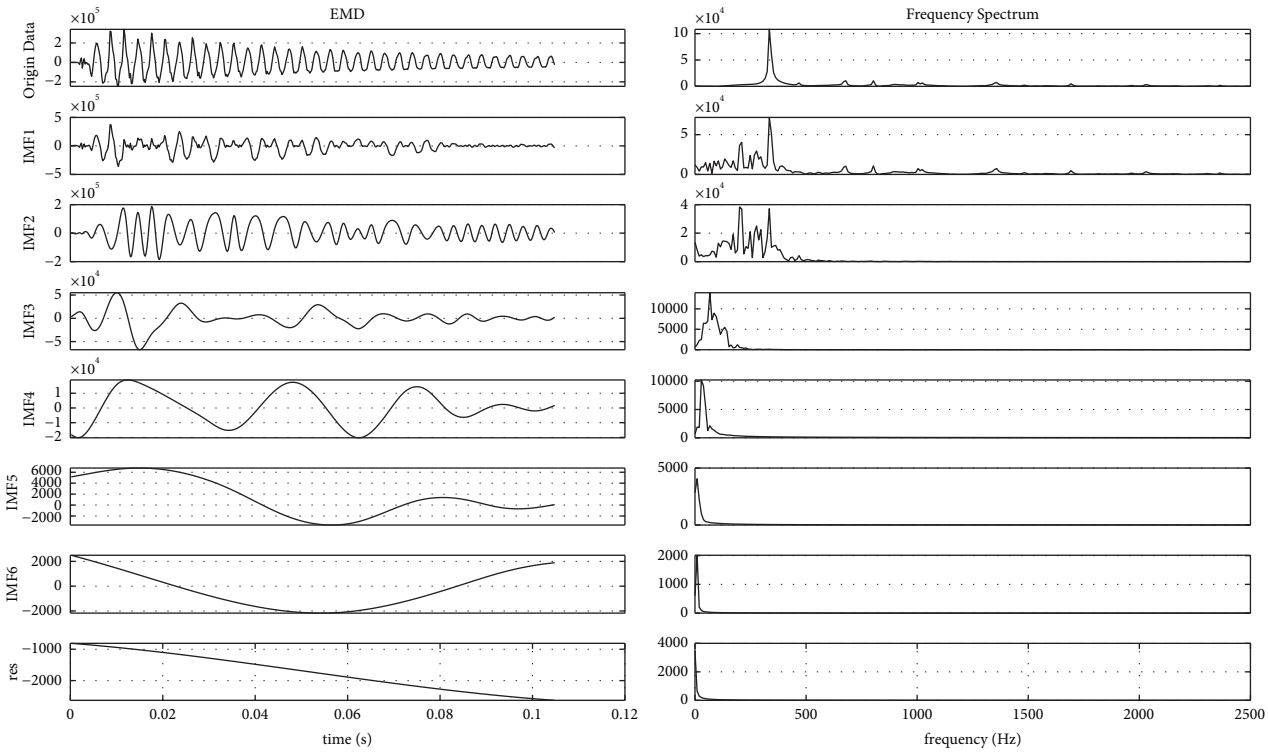

(b)

Figure 25: Continued.

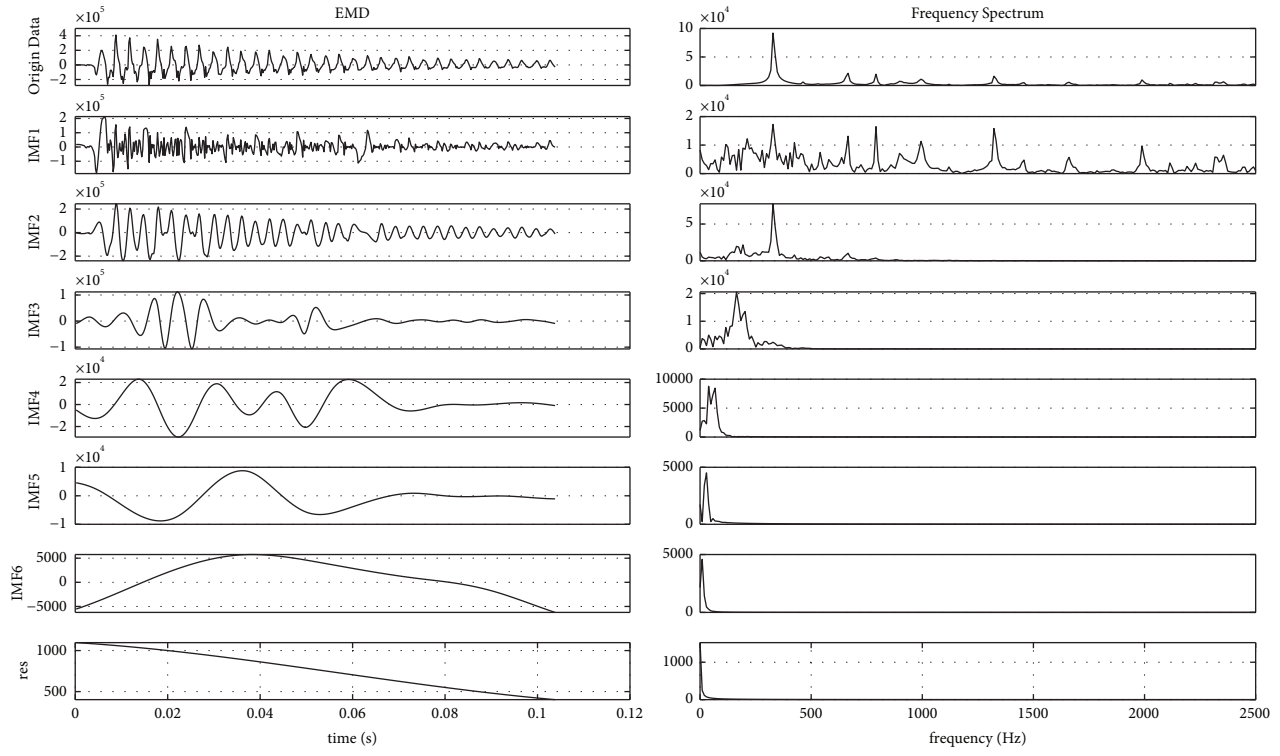

(c)

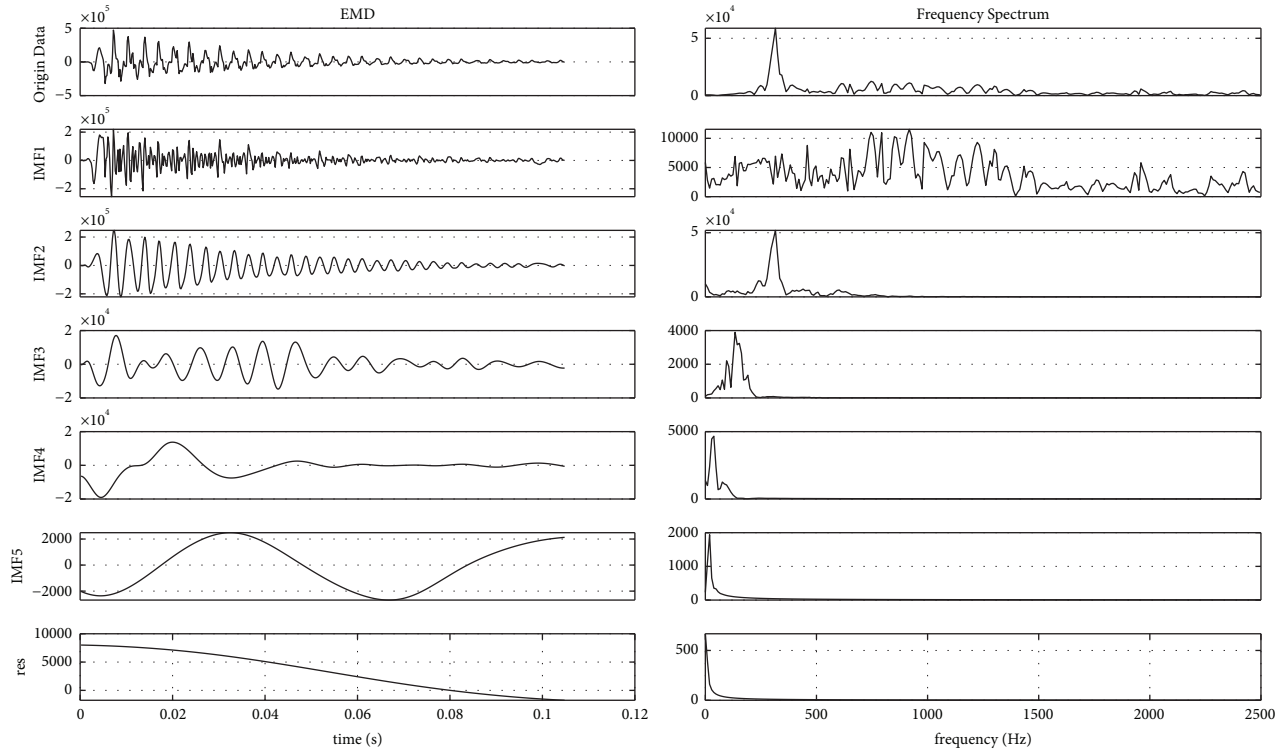

(d)

Figure 25: Acceleration signal EMD decomposition and frequency response curves of 6 bolts' flange structure under 1500 N impact load. (a) Tightening preload of 5000 N. (b) Tightening preload of 5000 N with one bolt loosened to 3000 N. (c) Tightening preload of 5000 N with one bolt loosened to 300 N. (d) Tightening preload of 5000 N with two adjacent bolts loosened to 300 N.

Table 3: Q_1 and ΔQ_1 of the connection structure with 6 bolts under 1500 N impact load with standard preload of 5000 N and different preload of loose bolt.

The test bolt preload	300 N (two loose bolts)	300 N	3000 N	5000 N
Q_1	5.52*E*6	4.42*E*6	1.94*E*6	1.64*E*6
ΔQ_1	2.37	1.70	0.18	—

Table 4: Q_1 and ΔQ_1 of the connection structure with 4 bolts under 1500 N impact with standard preload of 5000 N and different preload of loose bolt.

The test bolt preload	300 N	3000 N	5000 N
Q_1	1.58*E*6	6.79*E*5	4.84*E*5
ΔQ_1	2.26	0.40	—

Table 5: Q_1 and ΔQ_1 of the connection structure with 6 bolts under 1500 N impact load with standard preload of 4500 N and loose bolt preload of 300 N.

The test bolt preload	300 N	4500 N
Q_1	4.92*E*6	1.56*E*6
ΔQ_1	2.15	—

$$X(t) = \sum_{i=1}^{n} C_i(t) + r_n. \tag{3}$$

In equation (3), $X(t)$ is decomposed into n basic components $C_i(t)$ and a residual term r_n. Based on EMD and empirical mode decomposition, each order of IMF is obtained, and the original acceleration signal is decomposed. After the decomposition of the EMD algorithm, each order of the IMF is arranged from high frequency to low frequency, and different modal frequency bands are separated as much as possible. This paper employed an appropriate filter to process the IMF signal and obtain a specified frequency band signal for later analysis to eliminate moral ambiguity induced by the EMD method.

Finite Impulse Response (FIR) and Infinite Impulse Response (IIR) filters are commonly used filtering tools. Still, the frequency selectivity of FIR is not as good as that of IIR filters, and IIR filters contain feedback between the output and the input, and a smaller order can be used to meet the demand [38, 39]. Therefore, this article adopts IIR filter and Butterworth type as IIR method. Although the EMD algorithm has a certain filtering function, it makes the loosening index clearer and easier to judge. This paper uses IIR filters to further process high-frequency signals and separate high-frequency signals. The principle formula of IIR is as follows:

$$y(n) = \sum_{k=0}^{M} b(k)x(n-k) + \sum_{l=1}^{N} a(l)y(n-l). \tag{4}$$

In equation (4), $x(n)$ is the input signal and $y(n)$ is the output signal. The first accumulated sum is the M-section delay chain structure for the input signal $x(n)$, and $b(k)$ is the weight. The second part of the accumulated sum is the weighted addition of the delay of the output signal $y(n)$, where $a(l)$ is the weight.

Table 6: Q_1 and ΔQ_1 of the connection structure with 6 bolts under 1500 N impact load with standard preload of 4000 N and loose bolt preload of 300 N.

The test bolt preload	300 N	4000 N
Q_1	5.21*E*6	1.59*E*6
ΔQ_1	2.28	—

Table 7: Q_1 and ΔQ_1 of the connection structure with 6 bolts under 1000 N impact load with standard preload of 5000 N and loose bolt preload of 300 N.

The test bolt preload	300 N	5000 N
Q_1	2.65E6	1.10E6
ΔQ_1	1.41	—

Table 8: Q_1 and ΔQ_1 under different loose bolt preload of the connection structure with 6 bolts under 1500 N impact load with standard preload of 5000 N.

The test bolt preload	300 N	5000 N
Q_1	1.70*E*6	1.01*E*6
ΔQ_1	0.68	—

$$Q_i = \int_f \mathrm{imf}^i_{\mathrm{after-IIR-FFT}}, \tag{5}$$

$$\Delta Q_i = \frac{Q_i^{\mathrm{loosen}} - Q_i^{\mathrm{noloosen}}}{Q_i^{\mathrm{noloosen}}}. \tag{6}$$

Discrete integration is performed on the IIR filtered signal in the frequency domain to obtain the scalar value Q. In equations (5) and (6), imf is the vibration time-domain decomposition signal after EMD decomposition; i represents the i-th order decomposition signal. The imf first-order signal is used in this paper. The subscript after IIR-FFT indicates that the FFT transformation is performed after IIR filtering. The upper right subscript of Q_i indicates different bolt states. The integral sign indicates that the FFT transformed signal is integrated in the frequency domain.

By comparing ΔQ_1, the severity of loosening can be distinguished. The larger ΔQ_1 is, the higher loosening degree is. This article integrates this process into EMD-IIR-FFT (Discrete Integral) signal processing flow which can be packaged into an automated data processing flow to identify loosening. This is of great help to practical engineering applications.

Based on this process, the following loose identification process is established in Figure 24.

3.2. Simulations of Loosening Detection. To validate the proposed method, the typical connection structure containing fine bolt modeling is used in this subsection for

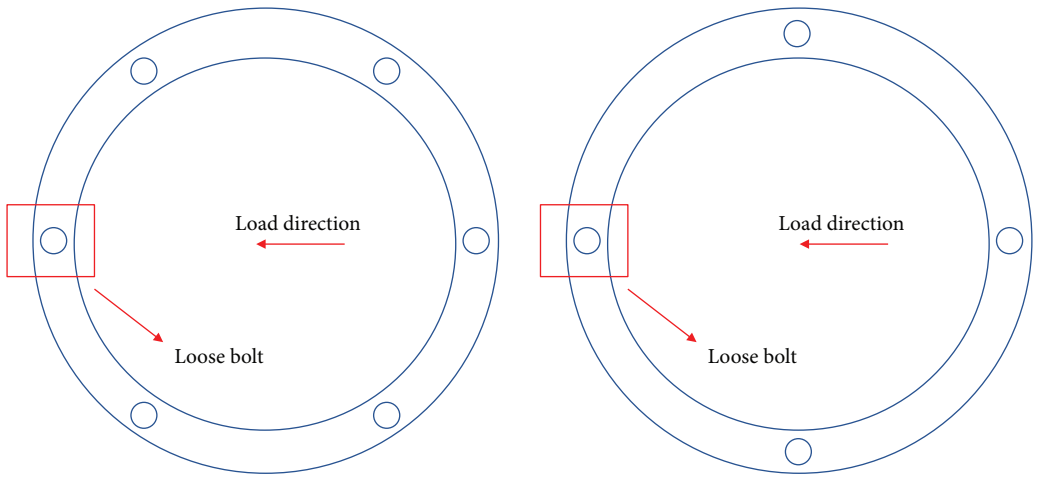

Figure 26: Schematic diagram of bolts arrangement in Tables 1 and 2.

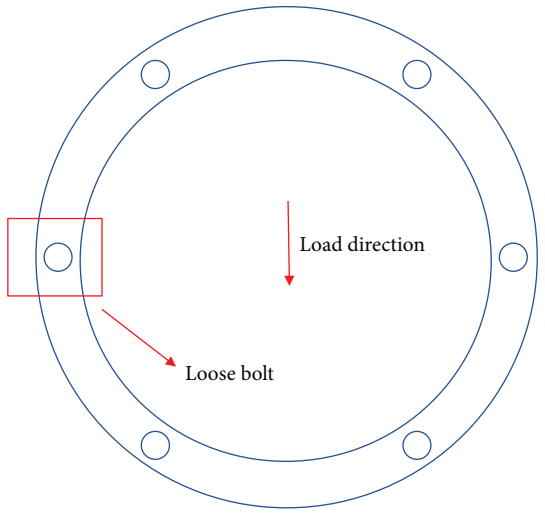

Figure 27: Schematic diagram of bolts arrangement in Table 6.

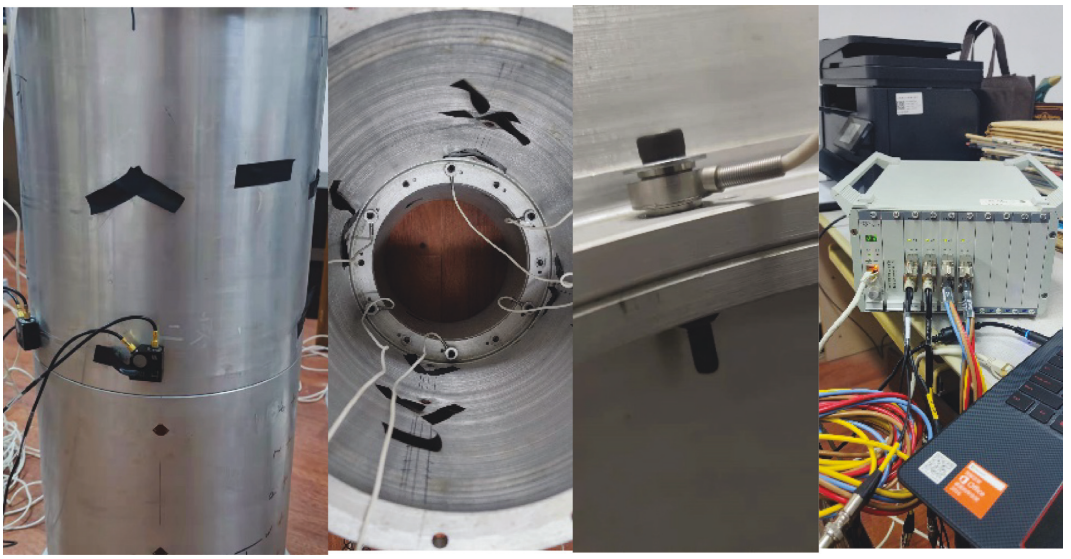

Figure 28: Experimental equipment.

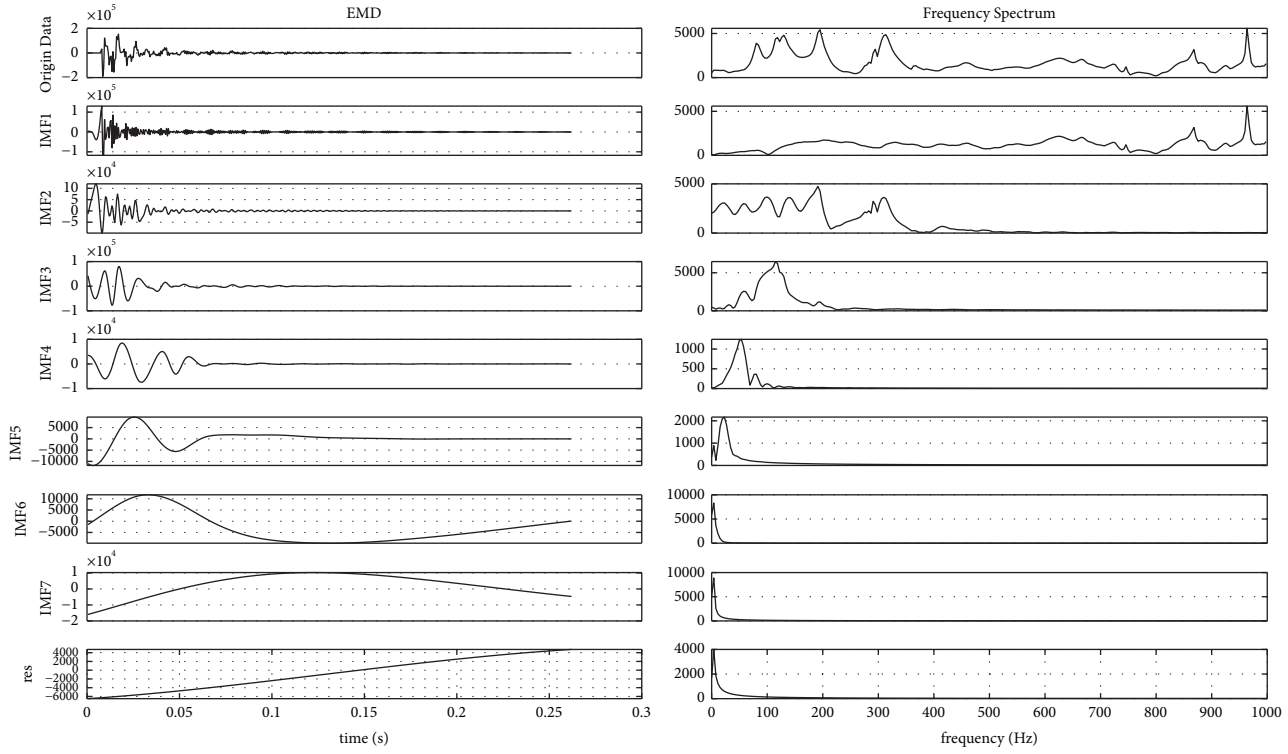

(a)

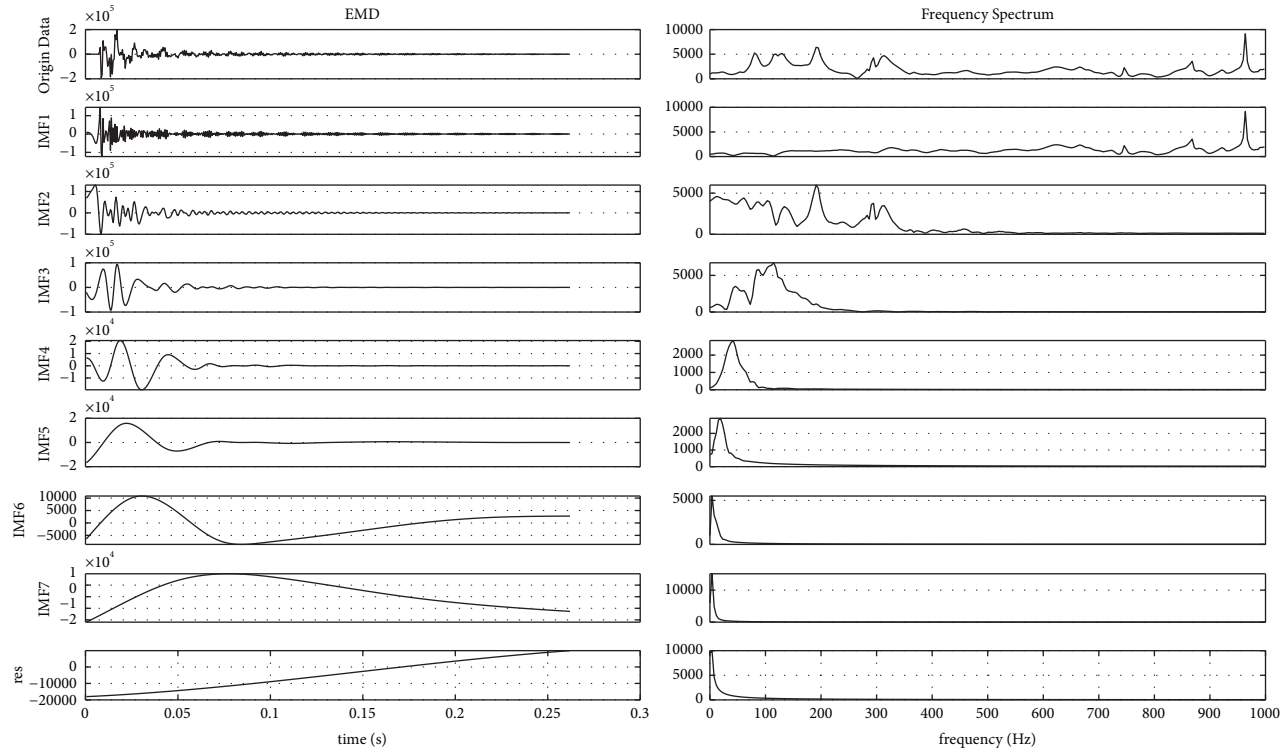

(b)

Figure 29: Continued.

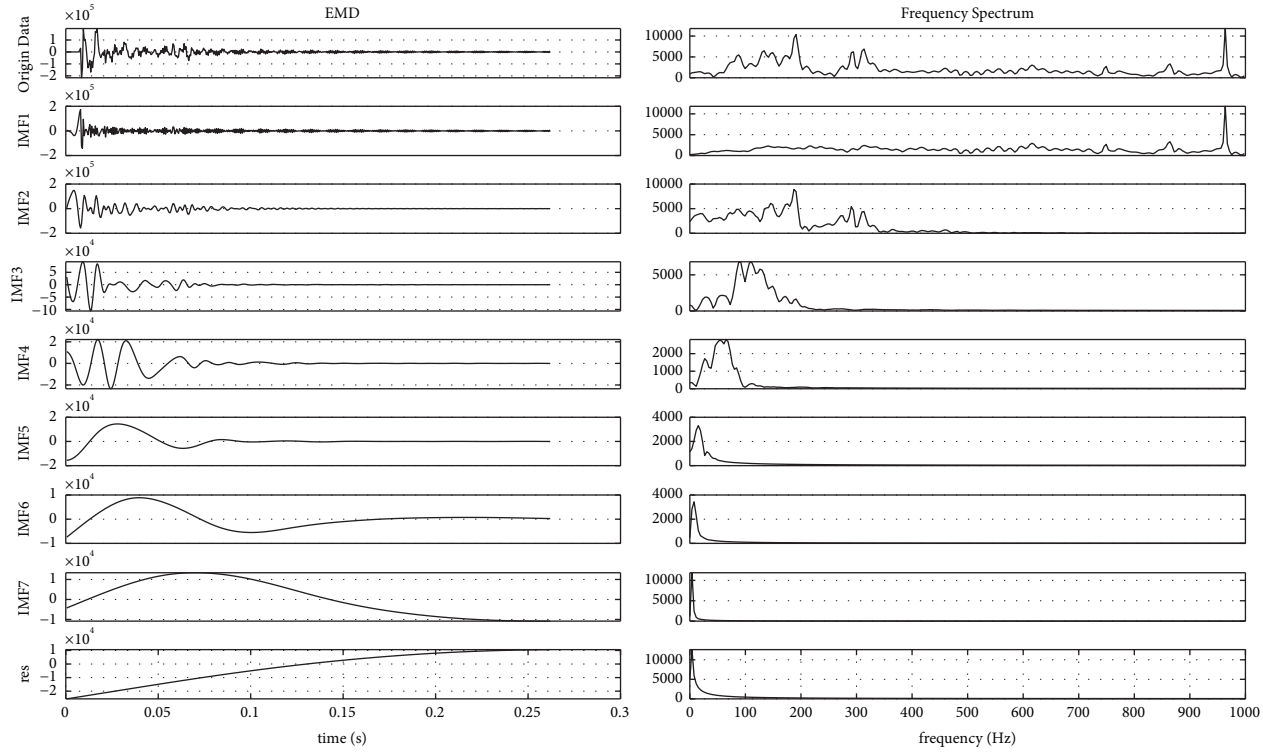

(c)

Figure 29: Acceleration signal EMD decomposition and frequency response curve. (a) Tightening preload of 5000 N. (b) Tightening preload of 5000 N with one bolt loosened to 3000 N. (c) Tightening preload of 5000 N with one bolt loosened to 300 N.

calculations at the level of finite element simulation. The same impact loads above were used to perform implicit dynamics calculations on the joint structure for different bolt preloads. The specific working parameters and dynamics setup parameters remain the same as in Section 2.2.2 of this paper, with only the preload level of the bolts being changed. Here different bolt preloads are used to characterize different degrees of bolt loosening conditions.

As shown in Figure 25, it can be seen that the complexity of the dynamic response signal does increase after the bolt is loose, with more frequency components appearing as the loosening increases. In particular, after the preload force is reduced to 300 N, the performance of the IMF1 (the first IMF component) is even more iconic and can reflect a significant nonlinear enhancement, which is consistent with the analysis. Although this signal has a certain specificity, it is still not intuitively simple and therefore the filtering mentioned above is necessary. Based on the established process, the filtered signal is FFT transformed and discrete integration is performed to obtain the results in the following tables (Tables 3–8).

The results in Table 3 verify the validity of the proposed method with Q_1 values increasing as the degree of loosening increases and ΔQ_1 values following the same pattern of variation. When even two adjacent bolts loose simultaneously, a significant increase in ΔQ_1 value is seen, which is consistent with the subjective judgement that the degree of bolt loosening has increased. Table 4 shows that the proposed method is equally applicable for connection structures

Table 9: Q_1 and ΔQ_1 under different bolt preload (impact experiment of the connection structure with 6 bolts).

Bolt preload	300 N (two loose bolts)	300 N	3000 N	5000 N
Q_1	3.92*E*5	3.20*E*5	1.93*E*5	1.47*E*5
ΔQ_1	1.67	1.18	0.31	—

Table 10: Q_1 and ΔQ_1 under different bolt preload (impact experiment of the connection structure with 4 bolts).

Bolt preload	300 N	3000 N	5000 N
Q_1	3.07*E*5	1.99*E*5	1.29*E*5
ΔQ_1	1.40	0.54	—

with varied numbers of bolts for the four-bolt arrangement of the flange connection structure in Figure 26. The Q_1 value has a scale, so its value is not important, whereas the ΔQ_1 value is a scale-free value and is therefore more important and accurate in determining loosening. Because the Q_1 value has such a big absolute value, the percentage rise in Q_1 value is not obvious even if the bolt is loose. When the bolt changes from slightly loose to almost fully loose, the ΔQ_1 value can vary by ten times, making it useful as a key indicator. When the ΔQ_1 value is close to 2, substantial bolt loosening occurs, as shown in the table above, which can be used as a criterion. When fewer bolts are used, the value of Q_1 is higher and the indicator is more sensitive. The proposed method is intuitive and simple for engineering application. As can be seen from

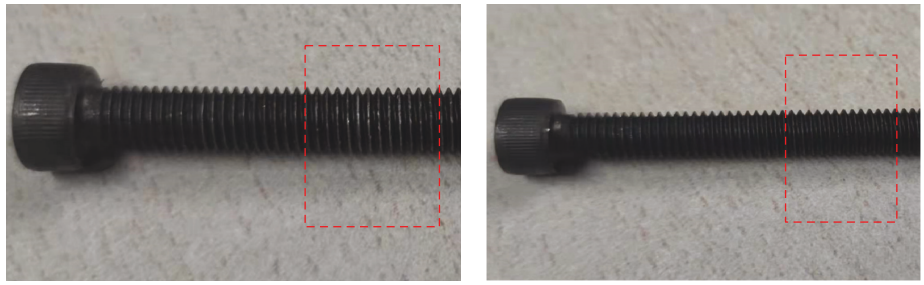

(a) (b)

Figure 30: Thread comparison. (a) A used bolt. (b) A new bolt.

Tables 5 and 6, the method is still valid for detecting loosening at different standard preloads, except that the ΔQ_1 value has some degree of variation. As can be seen from Table 7, the ΔQ_1 value becomes smaller as the load decreases to 1 kN, implying that the sensitivity of the indicator is positively related to the magnitude of the load. In the case shown in Figure 27, the direction of the impact load is perpendicular to the radial direction of the loose bolt. The Q_1 and ΔQ_1 values calculated according to the proposed method are shown in Table 8, which shows that the Q_1 values are significantly lower for the same degree of loosening. At the same time, the ΔQ_1 values are also reduced to a large extent. According to the results, it can be assumed that the smaller the angle between the direction of the impact load and the radial direction of the loose bolt is, the larger the ΔQ_1 value is, which is valuable for the subsequent development of this algorithm for determining the location of the loose bolt.

3.3. Experiment-Based Verification of the Loosening Detection. Impact experiments were conducted using a bolted flange connection structure presented in Section 2.1 to verify the effectiveness of the proposed loosening detection method. The acceleration response data was collected using a DH5922D vibration signal acquisition system in Figure 28. The bolt grade in the experiment was 12.9. Bolt pressure sensors were utilized to measure the preload to verify the same tension, with the impact load applied using a force hammer. To validate the proposed method, hammering experiments were conducted in loose and unloose conditions, and acceleration signals of the vibration were collected.

In the impact experiment, the connection structure with 6 or 4 bolts is subjected to a hammer impact of approximately 1000 N in three conditions: each bolt tightened with the preload of 5000 N, only one bolt loose to 3000 N, and only one bolt loose to 300 N. The signal was collected by an acceleration sensor and processed according to the designed procedure to obtain the results in Figure 29 and Tables 9 and 10.

The experiment shows in Tables 9 and 10 that the number of high-frequency components increases when loosening occurs as predicted by the proposed method. The value obtained in the experiment is not exactly the same as the value obtained by the finite element. This is due to the inevitable differences between the sampling rate and sampling duration of the actual experimental equipment and the finite elements. The signals received in the experiments are more interfering and do not agree exactly with the finite elements in terms of frequency components.

The finite element model is ideal, the contact surfaces are all flat, and only the linear friction relationship on the ideal contact surface is considered. However, the actual experimental conditions have complex friction relationships and have complex local warpage and wear conditions at the connecting contact surfaces. These differences in the discrete integration in the frequency domain make the ΔQ_1 values in error with the results obtained from the finite elements. Still, the trend is consistent where the greater the degree of loosening is, the higher the ΔQ_1 is, and the fewer the bolts are, the more sensitive the indicator becomes.

The difference between the Q_1 value in the finite element and the Q_1 value in the experiment is large, because the Q_1 value is dimensional, and the value of the discrete integral has a large difference due to the error mentioned above. Compared with the dimensional value, this paper focuses more on the dimensionless ΔQ_1 value. Based on the comparison of Tables 7 and 9, under the same six-bolt arrangement and 1 kN impact load, when severe bolt loosening occurs, the experimental ΔQ_1 value is 1.18, the finite element calculation ΔQ_1 value is 1.41, and the error is 16.3%. Whether it is the finite element results or the experimental results, the loosening of the bolt is quite serious when ΔQ_1 exceeds 1.

However, this experiment still proves that the bolt loosening can cause significant changes in high-frequency signals, which is enough to be applied to bolt loosening detection of actual structures and has certain engineering guiding significance. And as shown in Figure 30, it can be seen that the pretightened bolt has obvious wear at the thread, which is consistent with the result of the fine modeling above, which confirms that the modeling in this article reflects the situation that the traditional simplified modeling cannot respond before.

4. Conclusions

This paper simulates the contact properties of a typical bolted flange connection structure with pretightening bolts by the proposed FE model to investigate the impact

response. A novel bolt loosening detection method is developed. Based on the numerical and experimental cases, the following can be found:

(1) The modeling method for the bolted flange connection structure considering the detailed thread and pretightening process predicts the contact state and local stress more accurately.

(2) Under impact load, the local sticking contact area increases near the loose bolt of the bolted flange connection structure. Compared with a well-tightened one, the structure with loose bolt has additional high-frequency signals subjected to impact loads, which can become an effective approach to identify looseness.

(3) Through the analysis of the acceleration signals, the EIF data processing designed to identify loosening is established, and the method's effectiveness is verified through experiments. This proposed method can determine the occurrence of bolt loosening in the bolted flange structure nondestructively and quickly.

Data Availability

The data used to support the findings of the study are available from the corresponding author upon request.

Conflicts of Interest

The authors declare that there are no conflicts of interest regarding the publication of this paper.

Acknowledgments

The study was supported by National Natural Science Foundation of China (no. 11672052) and the Fundamental Research Funds for the Central Universities (DUT2019TD37).

References

[1] J. Kim, J.-C. Yoon, and B.-S. Kang, "Finite element analysis and modeling of structure with bolted joints," *Applied Mathematical Modelling*, vol. 31, no. 5, pp. 895–911, 2007.

[2] Y. Luan, Z.-Q. Guan, G.-D. Cheng, and S. Liu, "A simplified nonlinear dynamic model for the analysis of pipe structures with bolted flange joints," *Journal of Sound and Vibration*, vol. 331, no. 2, pp. 325–344, 2012.

[3] X. Lu, Y. Zeng, Y. Chen, X. Xie, and Z. Guan, "Transient response characteristics of a bolted flange connection structure with shear pin/cone," *Journal of Sound and Vibration*, vol. 395, pp. 240–257, 2017.

[4] T. Tian, J. Yuan, D. Li, Q. Wang, and B. Chen, "Study on the failure of the bolted flange connection structure between stages of missiles (rockets) under transverse impact load," *Shock and Vibration*, vol. 2018, Article ID 3953259, 16 pages, 2018.

[5] L. Zhu, A.-H. Bouzid, and J. Hong, "Numerical and experimental study of elastic interaction in bolted flange joints," *Journal of Pressure Vessel Technology*, vol. 139, no. 2, Article ID 021211, 2017.

[6] Y. Guo, Y. Wei, Z. Yang, C. Huang, X. Wu, and Q. Yin, "Nonlinearity of interfaces and force transmission of bolted flange joints under impact loading," *International Journal of Impact Engineering*, vol. 109, pp. 214–223, 2017.

[7] Q. Tang, C. Li, H. She, and B. Wen, "Modeling and dynamic analysis of bolted joined cylindrical shell," *Nonlinear Dynamics*, vol. 93, no. 4, pp. 1953–1975, 2018.

[8] Q. Tang, C. Li, and B. Wen, "Analysis on forced vibration of thin-wall cylindrical shell with nonlinear boundary condition," *Shock and Vibration*, vol. 2016, Article ID 8978932, 22 pages, 2016.

[9] C. F. Li, J. Yulin, Q. Ruihuan, and M. Xueyang, "Modeling and parameters identification of the connection interface of bolted joints based on an improved micro-slip model," *Mechanical Systems and Signal Processing*, vol. 154, Article ID 107514, 2020.

[10] C. Li, X. Miao, R. Qiao, and Q. Tang, "Modeling method of bolted joints with micro-slip features and its application in flanged cylindrical shell," *Thin-Walled Structures*, vol. 164, Article ID 107854, 2021.

[11] N. Jamia, H. Jalali, J. Taghipour, M. I. Friswell, and H. Haddad Khodaparast, "An equivalent model of a nonlinear bolted flange joint," *Mechanical Systems and Signal Processing*, vol. 153, Article ID 107507, 2021.

[12] F. Meisami, M. Moavenian, and A. Afsharfard, "Nonlinear behavior of single bolted flange joints: a novel analytical model," *Engineering Structures*, vol. 173, pp. 908–917, 2018.

[13] M. A. Beaudoin and K. Behdinan, "Analytical lump model for the nonlinear dynamic response of bolted flanges in aero-engine casings," *Mechanical Systems and Signal Processing*, vol. 115, pp. 14–28, 2019.

[14] G. Li, Z. Nie, Y. Zeng, J. Pan, and Z. Guan, "New simplified dynamic modeling method of bolted flange joints of launch vehicle," *Journal of Vibration and Acoustics*, vol. 142, no. 2, Article ID 021011, 2020.

[15] X. Jiang, Y. Zhu, J. Hong, X. Chen, and Y. Zhang, "Investigation into the loosening mechanism of bolt in curvic coupling subjected to transverse loading," *Engineering Failure Analysis*, vol. 32, pp. 360–373, 2013.

[16] S. A. Nassar and B. A. Housari, "Effect of thread pitch and initial tension on the Self-Loosening of threaded fasteners," *Journal of Pressure Vessel Technology*, vol. 128, no. 4, pp. 590–598, 2006.

[17] S. A. Nassar and B. A. Housari, "Study of the effect of hole clearance and thread fit on the Self-Loosening of threaded fasteners," *Journal of Mechanical Design*, vol. 129, no. 6, pp. 586–594, 2007.

[18] A. M. Zaki, S. A. Nassar, and X. Yang, "Effect of conical angle and thread pitch on the self-loosening performance of preloaded countersunk-head bolts," *Journal of Pressure Vessel Technology*, vol. 134, no. 2, pp. 566–571, 2012.

[19] T. Fukuoka, M. Nomura, and Y. Morimoto, "Proposition of helical thread modeling with accurate geometry and finite element analysis," *Volume 2: Computer Technology*, vol. 130, no. 1, pp. 135–140, 2008.

[20] Z. Chunjiang, L. Yongfeng, H. Xiaodong, G. Hailian, L. Yugui, and H. Qingxue, "Analysis of bearing characteristics of axially heavy-loaded composite nut," *The Journal of Strain Analysis for Engineering Design*, vol. 50, no. 5, pp. 325–334, 2015.

[21] S.-J. Chen, Q. An, Y. Zhang, and Q. Li, "Research on the calculation method of tightening torque on P-110S threaded connections," *Journal of Pressure Vessel Technology*, vol. 133, no. 5, Article ID 051207, 2011.

[22] T. Lin, R. Li, H. Long, and H. Ou, "Three-dimensional transient sealing analysis of the bolted flange connections of reactor pressure vessel," *Nuclear Engineering and Design*, vol. 236, no. 24, pp. 2599–2607, 2006.

[23] X. C. Liu, X. N. He, H. X. Wang, Z. W. Yang, S. H. Pu, and Z. Ailin, "Bending-shear performance of column-to-column bolted-flange connections in prefabricated multi-high-rise steel structures," *Journal of Constructional Steel Research*, vol. 145, pp. 28–48, 2018.

[24] Z. Wu, S. A. Nassar, and X. Yang, "Nonlinear deformation behavior of bolted flanges under tensile, torsional, and bending loads," *Journal of Pressure Vessel Technology*, vol. 136, no. 6, Article ID 061201, 2014.

[25] R. Grzejda, M. Warzecha, and K. Urbanowicz, "Determination of the preload of bolts for structural health monitoring of a multi-bolted joint: FEM approach," *Lubricants*, vol. 10, no. 5, p. 75, Article ID 10050075, 2022.

[26] A. Martowicz, A. Sendecki, M. Salamon, M. Rosiek, and T. Uhl, "Application of electromechanical impedance-based SHM for damage detection in bolted pipeline connection," *Nondestructive Testing and Evaluation*, vol. 31, no. 1, pp. 17–44, 2016.

[27] A. B. Thien, H. C. Chiamori, J. T. Ching, J. R. Wait, and G. Park, "The use of macro-fibre composites for pipeline structural health assessment," *Structural Control and Health Monitoring*, vol. 15, no. 1, pp. 43–63, 2008.

[28] B. Blachowski, A. Swiercz, P. Gutkiewicz, J. Szelążek, and W. Gutkowski, "Structural damage detectability using modal and ultrasonic approaches," *Measurement*, vol. 85, pp. 210–221, 2016.

[29] P. Becht, E. Deckers, C. Claeys, B. Pluymers, and W. Desmet, "Loose bolt detection in a complex assembly using a vibro-acoustic sensor array," *Mechanical Systems and Signal Processing*, vol. 130, pp. 433–451, 2019.

[30] R. Grzejda and A. Parus, "Health assessment of a multi-bolted connection due to removing selected bolts," *FME Transactions*, vol. 49, no. 3, pp. 634–642, 2021.

[31] B. Blachowski and W. Gutkowski, "Effect of damaged circular flange-bolted connections on behaviour of tall towers, modelled by multilevel substructuring," *Engineering Structures*, vol. 111, pp. 93–103, 2016.

[32] C. S. Patil, S. Roy, and K. R. Jagtap, "Damage detection in frame structure using piezoelectric actuator," *Materials Today Proceedings*, vol. 4, no. 2, pp. 687–692, 2017.

[33] H. Hasni, P. Jiao, A. H. Alavi, N. Lajnef, and S. F. Masri, "Structural health monitoring of steel frames using a network of self-powered strain and acceleration sensors: a numerical study," *Automation in Construction*, vol. 85, pp. 344–357, 2018.

[34] Y. Chen, Q. Gao, and Z. Guan, "Self-loosening failure analysis of bolt joints under vibration considering the tightening process," *Shock and Vibration*, vol. 2017, pp. 1–15, Article ID 2038421, 2017.

[35] Z. Li, Y. Chen, W. Sun, P. Jiang, J. Pan, and Z. Guan, "Study on self-loosening Mechanism of Bolted joint under rotational vibration," *Tribology International*, vol. 161, Article ID 107074, 2021.

[36] The Standard of People's Republic of China, "General Rules of Tightening for Threaded Fasteners," The Standard of People's Republic of China, Beijing, China, GB/T 16823.2-1997 in Chinese, 1997.

[37] N. E. Huang, Z. Shen, S. R. Long et al., "The empirical mode decomposition and the Hilbert spectrum for nonlinear and non-stationary time series analysis," *Proceedings of the Royal Society of London. Series A: Mathematical, Physical and Engineering Sciences*, vol. 454, no. 1971, pp. 903–995, 1998.

[38] S. Ocloo and W. Edmonson, "IIR filter adaptation using branch-and-bound: a novel approach," *IEEE Transactions on Circuits and Systems I: Regular Papers*, vol. 55, no. 11, pp. 3393–3403, 2008.

[39] S. R. Sutradhar, N. Sayadat, A. Rahman, S. Munira, A. K. M. F. Haque, and S. N. Sakib, "IIR based digital filter design and performance analysis," in *Proceedings of the 2017 2nd International Conference on Telecommunication and Networks (TEL-NET)*, pp. 184–189, Noida, India, August 2017.